Geographisches Institut | RWTH AACHEN UNIVERSITY

Diese Arbeit wurde vorgelegt am
Geographischen Institut
der Rheinisch-Westfälischen Technischen Hochschule Aachen

Bachelorarbeit

Relations between tree growth and carbon fluxes in the first decade of ecological forest conversion

Beziehungen zwischen Baumwachstum und Kohlenstoffflüssen im ersten Jahrzehnt eines Waldumbaus

von Anna Nele Hofer

407242 Umweltingenieurswissenschaften B.Sc.

Prüfer:
Univ.-Prof. Dr. rer. nat. Michael Leuchner
Dr. phil. Gunnar Ketzler

Aachen, den 26.04.2023

Abstract

Forests play a pivotal role in the global carbon cycle, acting as significant carbon sinks and influencing climate change mitigation strategies. This thesis investigates the relationships between tree growth and carbon fluxes within the ecological forest regeneration site of Eifel National Park over the period from 2016 to 2024. Utilizing eddy covariance measurements and forest inventory data, the study examines the correlations between net ecosystem productivity (NEP) and biomass increments of key forest species, including spruce (*Picea abies*), rowan (*Sorbus aucuparia*), and birch (*Betula spec.*).

The findings reveal strong relationships between growing season NEP from April to October and biomass increments for the species studied, indicating that higher NEP rates are consistently associated with greater biomass accumulation. The study demonstrated similar results for annual NEP from September to August and biomass increment. The relationship between biomass increment and NEP also suggests that spruce and rowan have a higher contribution to the NEP footprint than birch trees. Moreover, a higher correlation between the growing season NEP and the biomass increment of the population inside the protected area than for the population outside the protected area was found. Browsing on the trees outside the protected area may have affected the results.

It was found that only a small fraction of carbon influx during the growing season - ranging from 2.5 to 3.3 % - was stored in the aboveground biomass of the three studied species. The findings of this work underscore the need for continued investigation. Such research is very important to further improve the understanding of carbon dynamics. Further investigation will help in understanding the complex forest dynamics and carbon allocation patterns in the aboveground biomass formation of the study site.

Table of content

List of figures

List of tables

List of equations

List of abbreviations

CO_2 ..... *carbon dioxide*
EC ..... *eddy covariance*
FZJ ..... *Forschungszentrum Jülich*
GHG ..... *greenhouse gas*
GPP ..... *gross primary production*
IPCC ..... *Intergovernmental Panel on Climate Change*
NEE ..... *net ecosystem exchange*
NEP ..... *net ecosystem production*
NPP ..... *net primary production*
R^2 ..... *coefficient of determination*
RCP ..... *representative concentration pathway*
R_{eco} ..... *ecosystem respiration*
R_s ..... *soil respiration*

1. Introduction

Forests are significant atmospheric carbon sinks, that are crucial in the global fight against climate change. During photosynthesis trees absorb carbon dioxide (CO_2) and grow structural carbohydrates that comprise the wood matrix. The sequestered carbon is stored in wood fibers for decades to centuries before being released into the atmosphere through decay or burning (Foster et al. 2016). While globally 98 to 99.7 % of forests are net carbon sinks, 0.3 to 2 % of forests are carbon emitting (Körner 2003). As carbon uptake is a slow process, forest harvesting can release enormous amounts of carbon much quicker. A fire can release the carbon that has been taken up over 50 - 300 years in a matter of hours. When integrated across extended periods and large areas, uptake and emissions from these areas almost balance each other (Körner 2003).

Annual reports by the Intergovernmental Panel on Climate Change (IPCC) indicate the urgency to drastically reduce the net carbon emissions to zero to limit global warming to 1.5 or 2 °C (Lee and Romero 2023). By promoting the intact state of forests through sustainable management practices, reforestation, forest restoration and conversion, carbon storage can be enhanced (Lee and Romero 2023). Therefore, it is regarded as a negative emission technology, that can be employed as a nature-based approach by countries to partially reduce their carbon footprints. However, climate change and disturbances of flood, drought, fire or pest outbreaks impose an increasing threat to accumulated carbon in vegetation and soil (Lee and Romero 2023). According to Heilman et al. (2022) there is the possibility for an increase in carbon sequestration due to future elevated atmospheric CO_2 concentrations to a certain limit (Heilman et al. 2022). However, it is also possible that forests show a lower carbon uptake due to increasing drought stress and higher mortality (Heilman et al. 2022).

In Germany about a share of 32 % of the land is forested (BMEL 2021). In the last decade forest conversions funded by public funds have aimed to enhance forest resilience and biodiversity (BMEL 2021). Specifically, the growth of deciduous trees was promoted which made up a share of 55 percent in all forests in 2021 (BMEL 2021). The number of mixed forests has been increasing (BMEL 2021) with research suggesting diverse forests to enhance carbon storage (Bogena et al. 2015). Eifel National Park provides a good example of such an ecological transformation. Within the national park, a targeted intervention was strategically employed to promote the return to a more natural composition of tree species and structural diversity. The forest composition was converted from monoculture conifers to a more diverse and natural forest structure (Ney et al. 2019).

This thesis investigates the relationships between carbon fluxes and tree growth among specific tree species within the forest conversion site in Eifel National Park. Carbon fluxes obtained

through eddy covariance (EC) measurements and tree growth can be linked in order to improve the understanding of the forest carbon cycle (Teets et al. 2022). Soil studies can be a powerful additional tool to deepen the insights into forest dynamics, but are not considered here due to the scope of this work. This thesis should add to the understanding of forest dynamics for the regeneration area and the already existing research on the relations between carbon fluxes and tree growth, which has been a field of increasing importance.

As to the scope of this work, the most prevalent species have been selected to serve as a proxy for the relationships between carbon uptake and growth for the study site. These species are birch (*Betula spec.*), rowan (*Sorbus aucuparia*) and spruce (*Picea abies*).

To assess the relationships, the foundations required to understand the relationship between tree growth and carbon fluxes are provided at the beginning of the State of the Art chapter. This section provides a set of equations to estimate biomass growth based on the existing tree data. Moreover, current research in the field is displayed. Chapter 3 describes the study area and the input data, outlining the evaluation approach to assess the relationships between tree growth and carbon fluxes. The resulting datasets are presented regarding their imputation approaches as well as the resulting correlation analysis for height growth and biomass growth with carbon fluxes. Python is used for statistical and data analysis, providing insights into species-specific responses to environmental changes. These results are interpreted with regard to existing studies in the area as well as the limitations of this study. At last, further research perspectives are displayed. The most important findings are summarized in Chapter 5.

1.1 Goals

This study aims to contribute to the understanding of the forest dynamics of the ecological forest conversion in Eifel National Park. Utilizing forest inventory data and carbon flux measurements provided by the Forschungszentrum Jülich (FZJ), this work seeks to integrate and investigate the datasets comprehensively. As a part of this work, the author of this thesis has participated in collecting the current period's forest inventory data. The goal of this work is to explore the direct relationships between tree growth and carbon fluxes and to assess whether one variable can serve as a proxy for the other. In particular, this work aims at testing the hypothesizes that:

(i) an increase in CO_2 uptake is connected to enhanced tree growth, and
(ii) biomass increment is more accurate in describing the relationship between tree growth and carbon fluxes than height increment.

2. State of the art

This chapter provides a comprehensive review of the current knowledge and advancements in the field of forest dynamics. It lays a foundational understanding of the mechanisms that regulate tree growth and carbon fluxes. Additionally, background information on the study area along with research concerning the relationships between carbon fluxes and tree growth are presented.

2.1 Tree growth

This chapter provides the context for discussing biomass increments, describing the factors that influence tree growth and the methodologies employed to quantify biomass increments.

2.1.1 Environmental influences

Tree growth is a complex ecological process that is influenced by various factors such as temperature, precipitation, competition, tree size, tree age, soil quality and browsing. Browsing refers to the behavior of certain herbivores such as cervids to eat leaves, tree shoots or bark. These variables not only individually impact tree growth, but also interact with each other (Heilman et al. 2022).

According to Heilman et al. (2022) and Foster et al. (2016) there is a connection between water-year precipitation and maximum temperature such that a decline in growth occurs in years with high temperatures and dry conditions (Heilman et al. 2022; Foster et al. 2016).

In the absence of precipitation, small trees showed a greater decrease in growth; in contrast, larger trees were more susceptible to high temperatures. Moreover, trees with a bigger diameter experienced larger absolute growth reduction under high temperatures than trees with a smaller diameter. Heilman et al. (2022) demonstrated that canopy-dominating trees were more susceptible to temperature fluctuations, while trees with intermediate canopy levels were more sensitive to precipitation (Heilman et al. 2022). Specifically, hot future droughts could endanger canopy-dominant, high-biomass trees and cause stand-level losses in carbon storage, while droughts primarily driven by low precipitation could endanger small trees (Heilman et al. 2022). Moreover, they found higher fall-spring maximum temperature to have a strong negative effect and more water-year precipitation to have a positive effect on tree growth (Heilman et al. 2022). Foster et al. (2016) observed there to be a larger difference in growth response to mean annual temperature and summer moisture stress among individuals within a species than between species (Foster et al. 2016).

Neumann stated that the water supply in the growth-decisive period from April to July has a significant effect on tree growth. He concluded that the water supply during the vegetation period was the most important factor influencing the growth at a particular location for beech and spruce.

The comparison between beech and spruce shows that spruce is more sensitive to drought (Neumann).

Heilman et al. (2022) also suggest that there is an interaction between the site index and maximum temperatures, meaning that high temperatures at poor-quality sites have more detrimental impacts compared to high-quality sites (Heilman et al. 2022). Poor sites are locations that hold less favorable conditions for the selected tree species such as soil quality, moisture availability, nutrients, etc. The distinction between high and poor-quality sites is species-specific (Heilman et al. 2022).

Tree vulnerability to climate change seems to increase with more competition, tree size and poor sites. Interactions between site quality, competition and climate sensitivity can drive heterogeneity in climate responses of different forests. Disturbances by fire and insects are also likely to promote this (Heilman et al. 2022). Figure 1 demonstrates the set of environmental variables that influence tree growth.

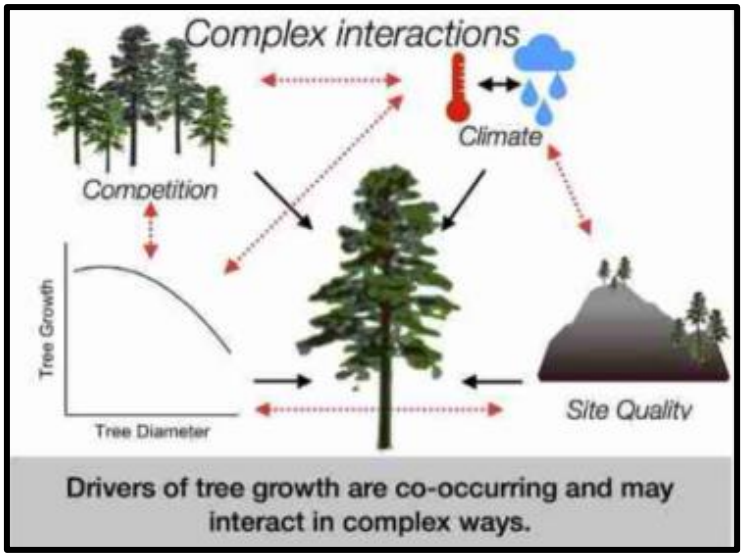

Figure 1: Environmental influences on tree growth (except from Heilman et al. 2022)

Heilman et al. (2022) also analyzed the impact of the various representative concentration pathway (RCP) scenarios on tree growth, concluding that with increasing warming (higher RCP scenarios) more trees are predicted to have a negative change in relative median growth (Heilman et al. 2022). The increased ability for carbon assimilation does not imply that biomass production and carbon storage increase adequately (Bartsch and Röhrig 2016), as the availability of other resources, suggests a higher impact (Heilman et al. 2022). The negative effects of warming are therefore expected to slow down the rate of tree-level carbon uptake and reduce carbon storage (Heilman et al. 2022). Foster et al. (2016) state that the growth of sugar maple, oak and spruce will vary more in the future in response to projected increases in annual temperatures and summer moisture stress (Foster et al. 2016).

For a global dataset, Foster et al. (2016) demonstrated that tree growth increases with tree size in terms of mass and carbon accumulation. Over time it is anticipated that older trees absorb less CO_2 (BMEL 2021).

According to the German forest report from 2021, there have been significant disturbances and damages to German forests as a result of the storms in 2017 and 2018, extreme drought and heat waves in 2018 to 2020 and the massive reproduction of the bark beetle. The climatic drought in 2018 was far more intense than the drought record year of 2003. The prolonged drought spanning three years resulted in previously unobserved desiccation of soil levels at depths exceeding one meter and a decrease in groundwater level (BMEL 2021).According to a risk assessment conducted by the Thünen Institute, current German forest stocks are especially vulnerable to aridity and drought events, particularly in areas where spruce or beech predominate (BMEL 2021). Spruce trees in particular suffered from poor water supply. In addition to drought and heat, parasite infection has been a major factor in tree mortality. In the future, efforts will be required to transfer monocultures not suited for the location into more natural mixed stands (BMEL 2021).

2.1.2 Allometric relationships and biomass calculations

Foster et al. (2016) state that tree growth is a multidimensional process characterized not only by diameter but also by volume and wood density. Tree diameter growth is correlated with an increment of biomass, however this relation is species-specific due to differences in stem geometry, stature and wood density and nonlinear (Foster et al. 2016).

Measuring the shift in the forest's biomass stocks serves as the foundation for determining energy wood potentials and the CO_2 sink capability. The biomass stocks are given in wood's dry mass and are used in greenhouse gas (GHG) reporting (Riedel and Kändler 2017).

In the German forest inventory report of 2021, equations by Riedel and Kändler (2017) are provided to determine aboveground biomass. This nationwide large-scale report is carried out every 10 years as stipulated by an amendment to the National Federal Forest Act. The function to estimate the aboveground biomass is comprised of three segments (Riedel and Kändler 2017, symbology part. adapted):

i. Trees ≥ 10 cm diameter at breast height (DBH) (based on data by Bösch et al. (2013):

$$Biom_{o,z} = b_0 e^{b_1 \frac{DBH}{DBH + k_1}} e^{b_2 \frac{d_{30}}{d_{30} + k_2}} {h_z}^{b_3} \quad (1)$$

with $Biom_{o,z}$ =aboveground biomass in kg per single tree, $b_{0,1,2,3}$ = coefficients of the Marklund function

The coefficients used in this equation are provided in Table 1. For trees with a DBH bigger than 10 cm, there is a distinction made between different tree species. Parameters for two deciduous

species (oak and beech trees) and two coniferous species (spruce and pine trees). Moreover, an additional group is provided for deciduous trees, which was obtained through measurements of birch, balsam poplar, alder, cherry, poplar, rowan, willow and other deciduous trees.

Table 1: Coefficients for biomass estimation for trees >=10 cm DBH, (Riedel and Kändler 2017,symbology part. adapted)

Tree Type	Category (computation)	b_0	b_1	b_2	b_3	k_1	k_2
Spruce	Fichte	0,75285	2,84985	6,03036	0,62188	42,0	24,0
Pine	Kiefer	0,33778	2,84055	6,34964	0,62755	18,0	23,0
Beech	Buche	0,16787	6,25452	6,64752	0,80745	11,0	135,0
Oak	Eiche	0,09428	10,26998	1,83894	0,55845	400,0	8,0
Deciduous trees	aln	0,27278	4,19240	5,96298	0,81031	13,7	66,8

ii. Trees ≥ 1.3 m in height and < 10 cm DBH (interpolation function):

$$Biom_{o,z} = b_0 + \left(\frac{b_s - b_0}{{d_s}^2} + b_3\,(DBH - d_s)\right) DBH^2 \qquad (2)$$

with $Biom_{o,z}$ =biomass in kg per single tree, $b_{0,s,3}$ = coefficients of the function and d_s= diameter measured at 30 % of tree height

This is an interpolation function between Equation 1 and Equation 3. The coefficients for this equation can be seen in Table 2. They follow the same distribution in groups for Equation 1.

Table 2: Coefficients for biomass estimation for trees >=1,3 m height and <10 cm DBH (Riedel and Kändler 2017, symbology part.adapted)

Tree Type	Category (computation)	b_0 in kg	b_s in kg	b_3
Spruce	Fichte	0,41080	26,63122	0,0136956
Pine	Kiefer	0,41080	19,99943	0,0091576
Beech	Buche	0,09644	33,22328	0,0116212
Oak	Eiche	0,09644	28,94782	0,0150098
Deciduous trees	aln	0,09644	16,86101	-0,0055086

iii. Trees < 1.3 meters height (based on actual data):

For calculation of the biomass of trees smaller than 1.3 meters, Riedel and Kändler (2017) distinguish in coniferous and deciduous trees.

This equation uses the coefficients provided in Table 3.

$$Biom_{o,z} = b_0 {h_z}^{b_1} \quad (3)$$

with $Biom_{o,z}$ =aboveground biomass in kg per single tree, $b_{0,1}$ = coefficients of the allometric function and h_z= tree height

Table 3: Coefficients for biomass estimation for trees <1,3 m height (Riedel and Kändler 2017, symbology part.adapted)

Tree Type	Category (computation)	$\mathbf{b_0}$	$\mathbf{b_1}$
Coniferous trees	Nadel (Fichte)	0,23059	2,20101
Deciduous trees	Laub (Buche)	0,04940	2,54946

Jumps between the functions have been eliminated in the transition zones and the criterion of continuity has been satisfied by statistically smoothing the functions. Figure 2 demonstrates the segmentation in biomass functions and the biomass progression according to the function used.

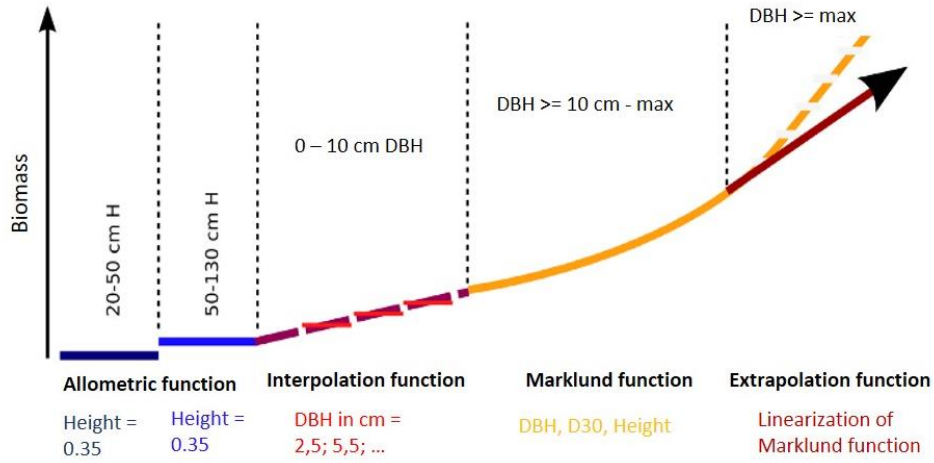

Figure 2: Segmentation of biomass functions (adapted from Riedel and Kändler 2017)

The BDAT3.0 program library can be used to calculate tree related data such as its dry volume and its diameter at a desired height by using the segmented biomass function (Riedel and Kändler 2017) It is available as an R-package on CRAN.

Wolff et al. (2009) introduce another function for the calculation of biomass specifically based on trees of regeneration areas, inherently young trees and shrubs with DBH smaller than 7 cm (Wolff et al. 2009). The data their function is based on, was obtained from trees of 46 Rhineland-Palatinate locations. The parameters used in their function are species-specific and are provided for several different coniferous (spruce, pine) and deciduous species (sycamore, birch, beech, rowan, oak, ash, buckthorn, broom and elder) (Wolff et al. 2009).

The biomass of an entire individual as well as the different plant compartments such as trunk, branches, etc. can be calculated according to Equation 4 (Wolff et al. 2009, symbology part. adapted):

$$Biom_{o,z} = e^{a} * d_{10cm}^{b} * h_{z}^{c} \quad (4)$$

with $Biom_{o,z}$ =aboveground biomass in kg, a, b, c= coefficients, d_{10cm}= diameter at 10 cm measured at 30 per cent and h_z= tree height

Table 4: Coefficients dry biomass single trees (excerpt from Wolff et al. 2009)

Tree species	Tree part	Height group	a	b	c
Birch	entire individual	all	-4,130332	1,851608	0,697924
		< 1m	-4,374745	1,952172	0,731565
		> 1m	-3,174592	2,680292	0,015936
Rowan	entire individual	all	-5,941790	1,212769	1,427108
		< 1m	-5,511373	1,102974	1,326973
		> 1m	-1.918987	1,599091	0,502464
Spruce	entire individual	all	-3,318449	2,008678	0,581185
		< 1m	-4,365029	1,873336	0,977148
		> 1m	-3,075020	1,605891	0,786470

By employing biomass functions the dry biomass of trees can be calculated, and transferred to estimate the carbon uptake via their carbon content. In 2017, German forests stored 2.6 billion tons of CO_2 in living biomass, deadwood and soil, living biomass accounted for 1.2 billion of this total (BMEL 2021).

2.2 Carbon fluxes

The carbon cycle is dynamic. Terrestrial biota recycle the amount of carbon stored in the atmosphere every 15 years (Körner 2003). Terrestrial and soil biomass store three times as much carbon as the atmosphere. As one-half of the terrestrial organic carbon is stored in forests, carbon release or uptake can significantly affect the atmosphere's CO_2 content. The carbon balance is crucial to the mitigation of climate change (Körner 2003). Because storage is also influenced by the residence period of carbon and the long-term dynamics of the forest, plot-based studies often overestimate the ability of forests for CO_2 uptake. With modern technology, CO_2 fluxes can be recorded. It is possible to continuously measure the net ecosystem exchange (NEE) rate per unit of land area (Körner 2003). NEE describes the vertical and lateral flux from the ecosystem to the atmosphere (Chapin et al. 2006).

The measured nighttime flux represents the ecosystem's overall respiration since photosynthesis stops during this period (Chapin et al. 2011). Ecosystem respiration is the total of respiration processes from all organisms in an ecosystem per unit of ground and time, which can be divided

into heterotrophic and autotrophic respiration. Gross primary production (GPP) and respiration rarely balance each other as photosynthesis typically surpasses respiration during daylight hours (Chapin et al. 2011).

NEE is subject to seasonal fluctuations, that vary across different ecosystems. Figure 3 demonstrates the seasonal fluctuations of NEE according to ecosystem type based on American vegetation sites in 2005. It shows that deciduous forests exhibited the most substantial negative NEE during the growing season, alongside the most positive NEE during the non-growing season (Xiao et al. 2008).

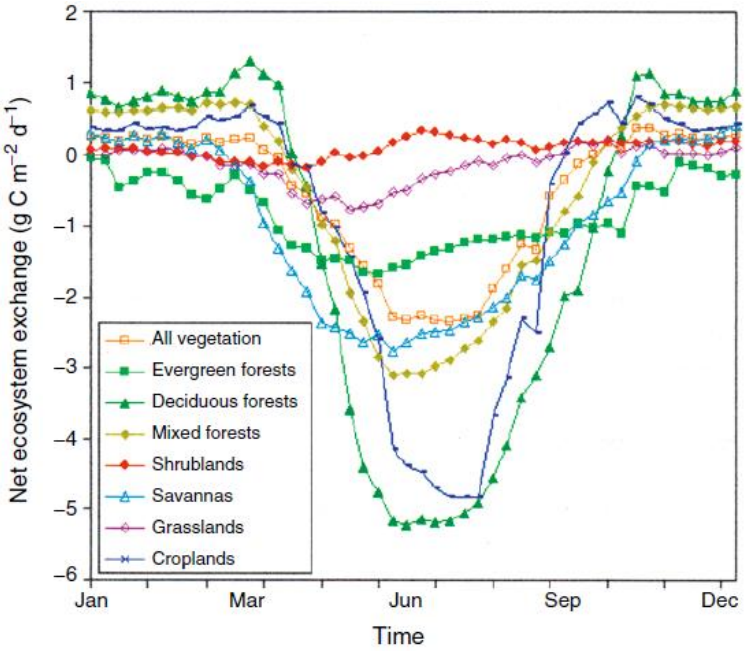

Figure 3: Seasonal patterns of NEE in different American vegetation types (as displayed in Chapin et al. 2011, adapted from Xiao et al. 2008)

The accuracy of NEE fluxes is comprised by atmospheric stability, which requires the inclusion of a correction term for storage and advection (Chapin et al. 2006). Factors like lateral air drainage at night can cause overestimation of NEE (Chapin et al. 2006). Moreover, it is suspected that carbon loss via harvesting, leaching and additional transfers play a significant role in the overall carbon balance of terrestrial ecosystems. Such non-gaseous forms of carbon loss are not captured in NEE measurements and often remain unquantified (Chapin et al. 2011).

The net ecosystem production (NEP) indicates the carbon input to the ecosystems as defined by ecologists, whereas NEE represents carbon input to the atmosphere as defined by atmospheric scientists (Chapin et al. 2011). The direct measurement of NEP (NEP= GPP – R_{eco}) is challenging in terrestrial ecosystems due to its complexity. Typically, it is estimated by NEE (Chapin et al. 2011).

NEP values are looked at from the forest pool perspective, therefore NEP fluxes approximated by NEE have the opposite sign to NEE (Teets et al. 2018). Carbon fluxes that are absorbed by the forest and accumulated have a positive sign, while carbon losses to the atmosphere are indicated by a negative sign (Teets et al. 2018). Discrepancies between NEE and NEP arise through leaching losses, that make the NEE values greater than NEP values (Chapin et al. 2011). In the growing season, NEP becomes positive as photosynthesis outpaces respiration, leading to biomass accumulation in plants. Conversely, in non-growing seasons, with reduced photosynthesis, heterotrophic respiration prevails, making NEP negative. This results in predictable daily and seasonal NEP patterns.

In southern Europe, GPP and ecosystem respiration (R_{eco}) are both significantly limited by moisture availability. In years or at sites with higher moisture levels, both GPP and ecosystem respiration increase similarly. Likewise, in northern countries, where temperature predominantly constrains GPP and ecosystem respiration, a rise in temperature during warmer years or at warmer locations causes similar increases in these processes. Spring warming can enhance GPP and NEP by hastening the snowmelt and the commencement of plant growth and photosynthesis. Conversely, during autumn, lower sun angles and warmer soil temperatures boost ecosystem respiration more than GPP, leading to a decrease in NEP during this season.

For the investigation of NEP fluxes, it is important to consider the reference period according to the investigation goal. Studies on tree responses to drought have employed the hydro-ecological year for the cumulative NEP fluxes per year (Teets et al. 2018). Other studies on the relationships between NEP and tree growth have employed different reference periods ranging from the calendar year to several months (Granier et al. 2008; Lagergren et al. 2019; Teets et al. 2018.; Teets et al. 2022).

Another approach is the use of growing season for cumulative NEP fluxes. Körner et al. (2023) highlight that there is no universally fixed definition for growing season and provide an overview of the different concepts along with their limitations (Körner et al. 2023).

Körner et al. (2023) categorize the definition of a growing season into four main concepts:

- Growing season *sensu stricto*: This definition refers to the period during which a plant actively grows and forms new tissue. It is characterized by the formation of new tissue and measurable increments in volume or dry matter.
- Phenological season: The growing season can be defined by phenological markers for growth. According to Körner et al. (2023), phenological markers are not always a reliable indicator for development.
- Productive season: This is the period during which the annual net primary production (NPP) or NEP is achieved. For this either NEE or NEP measurements or biomass

harvesting can be employed. Most commonly the harvesting method is employed, albeit it being more error-prone.

- Meteorological season: This period is a window of opportunity based on environmental conditions. It commonly makes use of ecologically relevant thresholds that usually refer to gradual changes such as spring warming, freezing or the mean annual temperature. However, these thresholds might not adequately reflect the variability in physiological responses across species and age.

Differentiating among these concepts is important as they influence the understanding and modeling of plant and biomass growth. Körner et al. (2023) highlight the need to distinguish between growth and development. noting the distinction between a net gain in dry matter and specific increments in plant organs, termed stored growth (Körner et al. 2023). The dynamics of root and rhizome formation remain often overlooked in actual growth activity and accumulated biomass, even though they play a pivotal role (Körner et al. 2023). Particularly in forests, there is an asynchrony between the aboveground and belowground biomass formation, with root activity commencing later and extending longer into the growing season (Körner et al. 2023).

2.3 Investigations of the study site in Eifel National Park

Ney et al. (2019) analyzed the carbon exchange in the forest conversion area in Eifel National Park, comparing the three years prior to partial deforestation in September 2013 to four years after (Ney et al. 2019). Within this area lies the study site, which was investigated in the following chapters.

Typically, forests in northern mid-latitudes serve as carbon sinks (Ney et al. 2019). However, disturbances such as clear-cutting, fire, insect outbreaks, and wind-throws can disrupt this balance and turn carbon sinks into carbon sources (Ney et al. 2019). Due to the clear-cutting of all spruce trees in the forest conversion area, natural gaps were formed and the soil was exposed. A soil exposure enhances the breakdown of soil organic matter, which emits CO_2 (Bartsch and Röhrig 2016).

During forest regeneration, the point when the ecosystem transforms from carbon-emitting to carbon-absorbing is called the carbon compensation point. The carbon compensation point varies between studies from 3 to 20 years covering a variety of climate conditions, forest ecosystems, stand age and post-disturbance land management (Ney et al. 2019). For changes and quantities of carbon in the soil, there are great uncertainties for analytical difficulties and correlated influences that change over time and in small locations (Bartsch and Röhrig 2016). The period until all the carbon that has been emitted has been absorbed after disturbance is referred to as the payback period. Aguilos et al. (2014) noted the payback period requires at least the same amount of time it needed for them to become carbon neutral.

The duration of these shifts varies based on the disturbance type, vegetation species, climate conditions and land management after the deforestation. Many studies have looked into these changes by using modeled or chrono-sequenced studies (Ney et al. 2019).

Research on different post-disturbance land management strategies has demonstrated that the transition of NEE from being a carbon source to a sink is not linear but fluctuates interannually (Ney et al. 2019).

In the first year after deforestation, the deforested area acted as a carbon source with positive NEE fluxes (Ney et al. 2019). As only 3 percent of aboveground biomass remained on site, it potentially limited the carbon emissions from decomposition. Due to low photosynthetic activity in the beginning years, the GPP fluxes stayed low (Ney et al. 2019). As vegetation began to recover, ecosystem respiration (R_{eco}) increased, together with an increase in GPP. R_s accounted for half the R_{eco} on the clear-cut site (Ney et al. 2019). Moreover, the daytime fluxes increasingly became negative. It is assumed that above and below-ground autotrophic respiration were key factors driving the surge in R_{eco}, while the rate of decomposition remained comparatively constant (Ney et al. 2019). Four years after deforestation, the area remained a CO_2 source with dynamic changes of NEE and GPP (Ney et al. 2019). In the subsequent years, there was a consistent decrease in NEE, showing a quick recovery of the area. During the beginning of the growing season of 2017 (May and June), it was noted that the deforested area saw a decline in GPP in combination with low air temperature and reduced precipitation, whereas the forested area in Eifel National Park saw an increase. Ney et al. (2019) concluded that the spruce forest has a higher resilience regarding its photosynthetic activity for shifting weather conditions compared to the grass-dominated clear-cut (Ney et al. 2019).

In 2021 the deforested area turned into a net carbon sink. The annual range for NEE measurements was between 545 g C m^{-2} yr^{-1} to -94 g C m^{-2} yr^{-1} from 2014 to 2023.

In combination with the EC measurements, soil respiration (R_s) was measured on-site using portable chambers, with the chambers closing for 90 seconds and using 60 seconds for flux calculation by fitting a linear regression to the empirical exponential van't Hoff equation to CO_2 concentrations.

As deforestation is expected to change a soil's chemical status due to the interconnectedness of water and biogeochemical nutrient fluxes (Bogena et al. 2015), changes in soil composition and water content were also assessed. These changes as reported in Bogena et al. (2015) are summarized here comprehensively together with the changes in albedo.

The soil water content changes were found to be strongest at the 5 cm depth, highlighting the topsoil's sensitivity to climate forcing. With even annual precipitation, significant variations in soil water content and groundwater depth were recorded from 2010 to 2013 (Bogena et al. 2015).

Following deforestation, the albedo for the deforested area increased from 16 to 25% in the first three years (Ney et al. 2019). This increase was initially driven by the regeneration of the site from bare soil to the growth of grass and shrubs. In the fourth year, the albedo decreased with the growth of rowan and broom vegetation (Ney et al. 2019). The associated cooling effect through the increase in albedo outweighed the warming effect of NEE (Ney et al. 2019). The albedo of the deciduous forest can be expected to remain higher than that of a spruce forest (Ney et al. 2019).

2.4 Current status of research

There have been different studies in the field of analyzing the relationships between carbon uptake and tree growth. Biomass herein was obtained through biomass functions that used the diameter measurements as a predictor of biomass. In the studies, tree dendrometers were used for measuring tree diameters and NEE measurements were employed for NEP fluxes. The investigated ecosystems were North American temperate and boreal forests (Teets et al. 2018; Teets et al. 2022) and different European boreal forests (Granier et al. 2008; Lagergren et al. 2019; Teets et al. 2018).

The study by Teets et al. (2018) on a mixed coniferous American forest was the only study to use a long-scale period of 20 years. The others mostly investigated periods of 10 years (Teets et al. 2022.; Granier et al. 2008; Lagergren et al. 2019). Their findings suggest delays in carbon allocation, as most of the referred studies observed strong relationships for lagged NEP or several month-long period of NEP with biomass increment (Teets et al. 2018; Teets et al. 2022.; Granier et al. 2008; Lagergren et al. 2019). For NEP cumulated for the calendar year, most correlation analyses showed weak relationships between NEP and biomass. Their findings are contextualized within the study's findings and are compared to my results in Chapter 4.4.

3. Material and methodology

3.1 Study area

A terrestrial network of observatories (TERENO) was set up in Germany to generate long-term data on ecosystem states and fluxes to study and predict the effects of climate and land use change. Another goal is the development and implementation of comprehensive model systems to employ more effective strategies for prevention, mitigation, and adaptation to the impacts of global change (Bogena et al. 2015).

The Wüstebach catchment is part of the TERENO network and situated in the Eifel National Park (Bogena et al. 2015). It is close to the border between Germany and Belgium and encompasses an area of roughly 38.5 hectares. The elevation ranges from 595 to 630 meters (Bogena et al. 2015). The average slope of the area is 3.6 % (Ney et al. 2019). The predominant soil types in this region are gleysols, with some areas of cambisols. In alignment with the national park's forest management objective to promote the natural regeneration of semi-natural beech forests, a substantial portion of the spruce forest, originally established post-World War II for timber production, was removed. In early autumn 2013, all spruce trees across a nine-hectare area were cut down (Bogena et al. 2015).

Figure 4 provides an overview of the Wüstebach catchment. The ecological forest conversion site studied in this work is positioned within the area depicted in yellow.

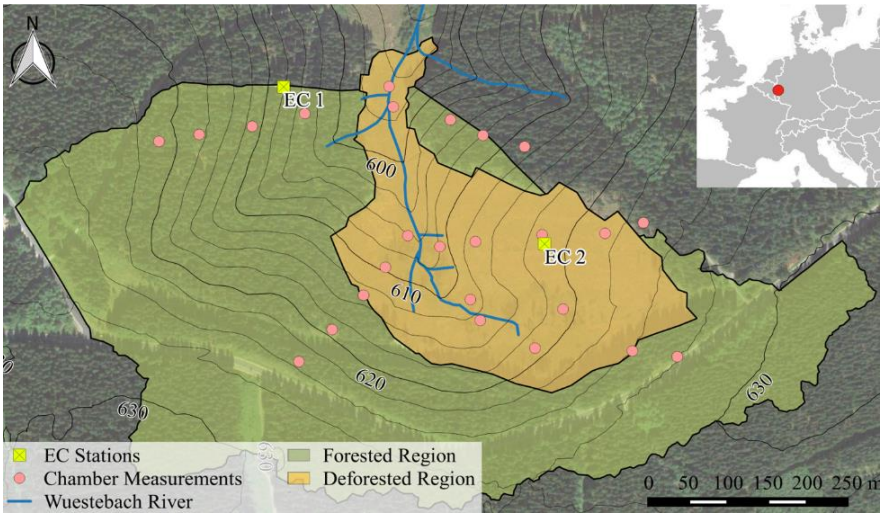

Figure 4: Map of the Wüstebach catchment (Ney et al. 2019)

Before clear-cut, it was predominantly covered by 70-year-old Norway spruce with an average height of 25 m. After clear-cutting using a cut-to-length method only three percent of the original biomass was left on site. In the initial years after deforestation, mainly grasses, red foxglove, and fireweed started to grow in the area, followed by the emergence of new trees such as rowan, spruce, birch, aspen, elder, and shrub vegetation including broom, heather, European blueberry

and bulrushes at the edges of Wüstebach (Ney et al. 2019). For this study, a site within the deforested area was chosen. This area lies within in 10-meter buffer relative to a fence that was set up to analyze the impact of wildlife on vegetation growth. The study area is shown in Figure 5, displaying the investigated areas inside (green) and outside (yellow) relative to the fence.

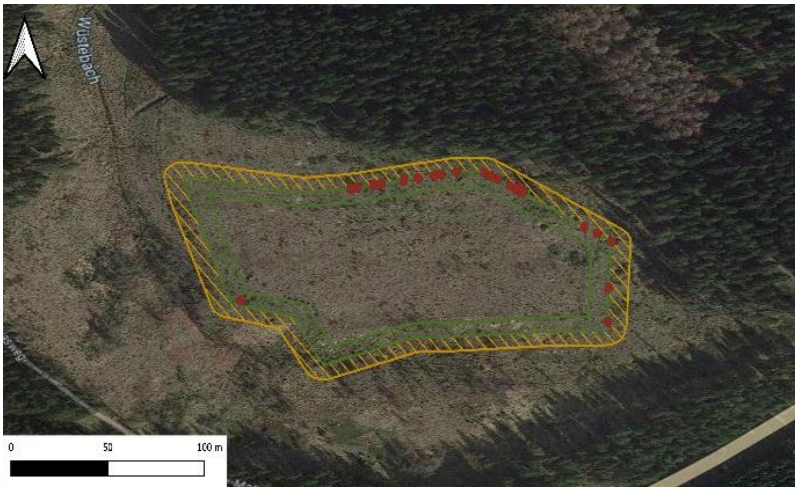

Figure 5: Study area separated into the area outside (yellow) and inside (green) the fence, the brown dots demonstrate the fence pillars that were GPS referenced (Source: Google)

The long-term precipitation history for the Wüstebach catchment can be approximated using measurements from the Kalterherberg meteorological station, which is located 5 km west of the site (Ney et al. 2019). The study area experiences moderate winters with snow for about 50 days (coverage of >= 50 %) per year and a mean snow depth of 13 cm, while summers are cool and relatively humid. Precipitation is evenly distributed throughout the year, with peaks in winter and summer months as a result of frontal and convective weather patterns. The wind predominantly comes from the southwest (Bogena et al. 2015).

3.2 Biometrical tree measurements

The data for the forest inventory of the Wüstebach catchment was obtained through field visits. In January 2015, the height measurements of trees in the study area was initiated. Every year, this tree data is updated with new measurements during the current non-growing season by Forschungszentrum Jülich (FZJ). At the time of the initial recording, trees are assigned a unique ID and recorded with their GPS coordinates on the nine-hectare plot. This allows the identification and continuous measurements of recorded trees over several years. In the initial years of the forest inventory, all trees and shrubs were recorded. After 2017, the measurements were limited to trees located within a 10-meter buffer on either side of the fence. Since 2016, the species of the tree, growth form (number of trunks) and partly diameter at a height of about 10 cm were recorded. From 2021, the dataset was expanded to include the diameter at breast height (DBH) for each tree. DBH is recorded in a height of 130 centimeters. Part of this work was also the measurement of tree heights and diameters from January to March 2024 and the evaluation of

the complete dataset from 2015 to 2024. Both electric and mechanical calipers were used for diameter measurements. The heights were measured using a rod. During the measurements in the winter of 2022, it was found that some trees had grown beyond four meters, which exceeded the capacity of the initial rod. As a result, trees taller than four meters were not recorded in the winter 2022 to 2023. Consequently, in 2022 a big number of birch trees uniformly lacked height data, whereas their breast height diameters were assessed. In the measurements in winter 2023, a newly acquired longer rod was used, that was capable of measuring taller trees. This new rod is depicted in Figure 6.

Figure 6: Measurements for the forest inventory using the mechanical caliper and newly acquired rod (Source: Alexander Graf 2024)

It is to be expected that both methods exhibit measurement inaccuracies, due to errors in reading or applying the measuring stick or caliper. Additionally, measurement errors were observed when using the electronic caliper in January 2024, which presumably could be related to the moisture sensitivity of the electronic caliper. After that, work was carried out exclusively with the mechanical caliper. Past records do not indicate which measurements were performed with mechanical calipers and which with electronic calipers.

3.3 CO_2 flux measurements

The provided data of carbon fluxes by the FZJ was obtained by using the eddy covariation station in the study area. Eddy covariance (EC) is a micrometeorological measurement method that quantifies the turbulent fluxes in the near-surface atmosphere with the net transports of energy, water and gas exchange (Bartsch and Röhrig 2016). It assumes that vertical fluxes are based on eddies, spatially confined turbulences that can be determined from vertical wind speed, temperature and humidity (Bartsch and Röhrig 2016). CO_2 fluxes are calculated by analyzing the timing and instantaneous variations in CO_2 levels and vertical wind speeds as turbulent eddies

move past the sensors (Chapin et al. 2011). Summing these flux measurements over an hour, a day, or a year provides a comprehensive view of the net CO_2 exchange between the ecosystem and the atmosphere for the specified duration. The ecosystem's CO_2 intake is defined as negative NEE (Chapin et al. 2011). If the NEE is positive, carbon is emitted from the system (Körner 2003). The EC-generated NEE is most precise for short-term estimates as environmental variability such as weak turbulences and precipitation, as well as the integration of daytime and nighttime measurements, can introduce measurement errors (Reichle 2020). The eddy covariance method is employed in terrestrial ecosystems both within and above the vegetation zone for total system fluxes (Reichle 2020).

Since September 2013, an EC station has been operational in the center of the deforested area, positioned 2.5 meters above the ground to reduce the influence of the surrounding terrain (Ney et al. 2019). The EC station is positioned within the deforestation area (displayed in yellow) inside of the depicted isolines, which can be seen in Figure 7**Fehler! Verweisquelle konnte nicht gefunden werden.**. According to Ney et al. (2019), the footprint of the EC- station fits with the shape of the deforested area, as the 90 % isoline of the EC footprint is almost completely located within the boundaries of the deforested area (Ney et al. 2019).

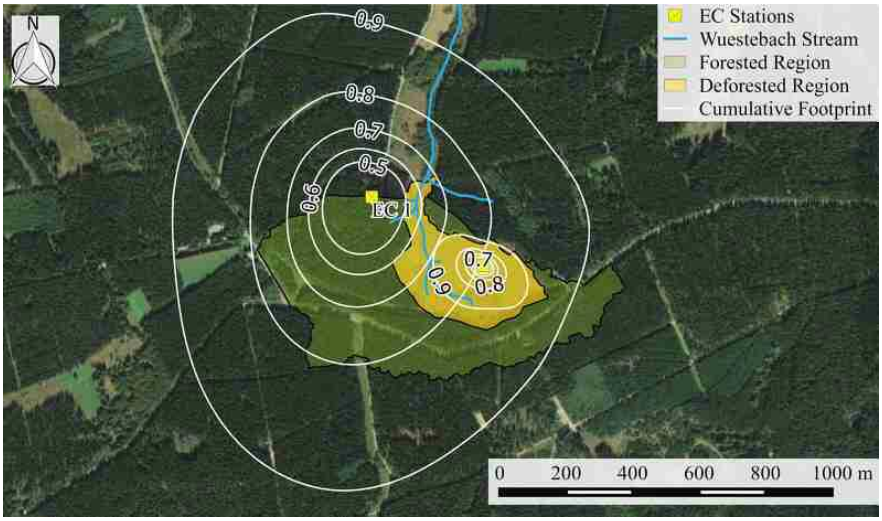

Figure 7: Cumulative footprint for the forest EC stations within the forested area (EC 1) and the deforested area (yellow area). The EC in the deforested area is within the 0.7 isoline of the yellow area. The 0.7, 0.8 and 0.9 isolines equal 70, 80 and 90% of source distribution. (Ney et al. 2019)

THE EC station measures the 3D wind vectors, temperature, humidity, and CO_2 levels at a 20 Hz frequency. A Campbell Scientific CSAT3 sonic anemometer is employed for wind speed and direction and a LiCor Li-7500 open-path gas analyzer, is placed 15 cm north of the anemometer, to assess the gas concentrations (Bogena et al. 2015). Both instruments are attached to a 1.5-meter boom oriented at 182° (Bogena et al. 2015). Turbulent fluxes of heat, momentum, CO_2, and water vapor are computed with the TK3 software (Mauder et al. 2013). The measurement height was repeatedly adapted to the growth of the canopy, including a period of simultaneous

measurements at two levels (Reitz et al. 2022). Occasionally supplementary manual measurements of CO_2 flux and evapotranspiration were performed to ensure the EC station's data accurately reflects the small deforested area (Bogena et al. 2015).

The influence of the forest edge on the flux measurements of the clear-cut is also assumed to be minimal (Ney et al. 2019). When working with NEE fluxes obtained by the EC method, there may be inaccuracies. Even under otherwise ideal conditions, it is common for EC measurements to have an imbalance of 20 % when comparing the obtained turbulent fluxes with the available energy (Ney et al. 2019).

During stable conditions, storage fluxes and advection become critical, especially in tall canopies and complex terrains. This issue, often referred to night flux error, leads to an underestimation of CO_2. Even though it is possible to reduce the night flux error by discarding nighttime data affected by low turbulence, this might still result biased results (Ney et al. 2019).

3.4 Evaluation approach

Addressing missing data in datasets is a significant challenge. Deleting cases with missing values, results in increased uncertainty and biased parameter estimates (Nakagawa and Freckleton 2011). In the forest inventory of a regeneration site, missing values arise due to various factors. These include the inability to locate certain trees, tree mortality over the observation period and asynchronous growth patterns. Consequently, the number of trees measured each year is not a constant. As the vegetation consisted mainly of shrubs and a small number of trees shortly after clear-cut, tree data in 2014 and 2015 was notably scarce. Therefore, the observation period was set between 2016 and 2024. Considering this, three different methods have been adopted to use the tree data for correlation analyses:

- Naive approach: This method uses recorded trees within the ten-meter buffer relative to the fence throughout the observation period. This dataset varies in size across the different years.
- Cleaned approach: This method selects only trees consistently present in every observation period to ensure dataset uniformity. For this approach, incomplete tree growing sequences are generously removed, excluding any trees that lack height data in at least one year.
- Filled Approach: The approach addresses missing height data through imputation by filling these gaps to maintain the completeness of the dataset. The imputed values are calculated by detecting a tree that matches the growth pattern of the tree with missing height data. Only trees of the same species are used for height imputation using a linear regression of the height data of the considered trees. In the correlation analyses, this is referred to as the filled dataset.

A bivariate correlation analysis is conducted using NEP fluxes obtained by NEE measurements and tree growth data. The Pearson correlation is employed, which is used to examine a linear relationship between two interval-scaled variables. A positive correlation indicates that a high expression of one variable aligns with a high expression of another variable, and similarly for low values. A negative correlation suggests that high values of one variable correspond to low values of the other. This method examines the undirected relationship between variables, without causal statements on the dependency of one variable to the other. The correlation coefficient ranges between -1 and +1. Values around 0 indicate that there is no relationship between the analyzed variables.

To prove a Pearson correlation, it is necessary to have variables that are at least interval-scaled and normally distributed, as well as a linear relationship between the two analyzed variables (HSLU Hochschule Luzern).

The Pearson correlation coefficient r is described by the following equation:

$$r_p = \frac{\sum_{i=1}^{n}(x_i - \bar{x})(y_i - \bar{y})}{\sqrt{\left(\sum_{i=1}^{n}(x_i - \bar{x})^2\right)}\left(\sum_{i=1}^{n}(y_i - \bar{y})^2\right)} \quad (5)$$

with x_i, y_i = variables of the variables x and y, $\dot{x}, \dot{y}$ = mean values of the variables x and, n= number of data points

In a different approach, the Spearman correlation coefficient r_s has been studied. It can be described by the following equation (Martin 2012):

$$\rho_R = 1 - \frac{6}{n\,(n^2 - 1)} \sum_{i=1}^{n} d_i^2 \quad (6)$$

with n = number of data points and d_i the differences in the ranks of x_i and y_i

Differing from the Pearson coefficient, the Spearman coefficient ρ_R is a rank correlation coefficient that uses the rankings of the variables x and y instead of their numerical values. Thus, this method can be used without assumptions regarding the distribution of the analyzed variables. (Martin 2012)

In order to investigate the relationships between CO_2 flux and tree growth, correlation analyses between the growth of three selected tree species and the CO_2 fluxes are performed. For this, NEP fluxes paired with tree growth data both in terms of height growth and biomass increment from the forest inventory are used. The final evaluation was conducted before the tree measurements were finalized for the growth period of 2023. When comparing the average number of trees measured over the past three years with the number of trees recorded for this growth period, 87.5 % of trees were included. Due to the large size of the datasets, Python (version 3.11) was utilized within a Spyder environment.

4. Results and discussion

In the subsequent section, a distinction between the methodologies is made, followed by the presentation and comparison of the results derived from the different approaches. For reasons of clarity and logical flow, the results of this study are directly followed by a discussion within the same section. The integration of the discussion within the results section facilitates a more seamless synthesis of the conclusions and supports the establishment of clear linkages between the findings and their context.

4.1 Datasets of tree measurements and carbon fluxes

This section describes the resulting datasets, outlining the differences, which might subsequently influence the outcomes of the study.

4.1.1 Tree data

Three approaches were implemented to deal with missing tree data. The naive dataset comprised a total of 1905 trees, representing all trees assessed within the defined study period from 2015 to 2024 within the final study area (10 meters to each side of the fence). The composition of tree species according to this approach can be seen in Figure 8, consisting of 1380 rowan trees, followed by 184 spruce trees, and 152 birch trees.

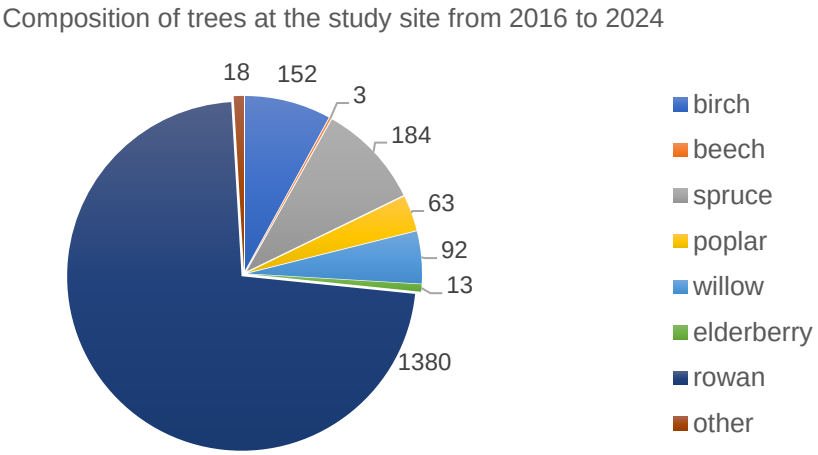

Figure 8: Composition of tree species at the study site during the period of investigation (all tree species with a population <5 individuals are included in "other")

Browsing had a strong effect on tree growth for several species. Figure 9 illustrates the height growth of the most common trees during the investigated period.

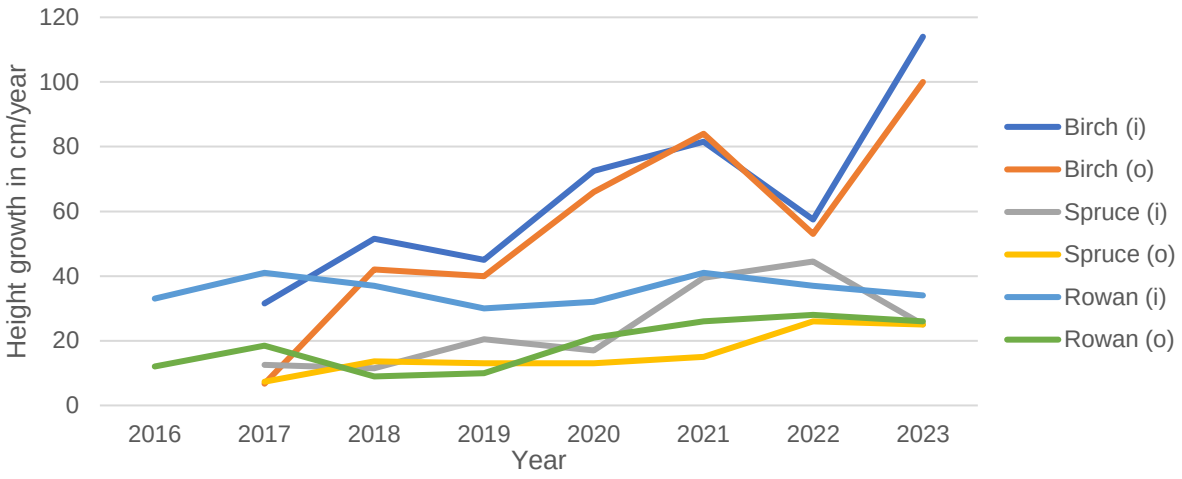

Figure 9: Absolute median height growth per selected group (filled dataset)

Trees inside the fence exhibited substantially higher growth compared to those outside. This contrast was found to be the highest for rowan trees. A similar pattern was noted for birch, even though the difference in height growth over the years varied. Spruce trees showed notable differences in growth rates for all years except 2017 and 2023. In 2023 this might be linked to the logging activities in the national park in the last year, which might have led to a focus on smaller spruce trees in the measurements.

As can be seen in Figure 9, both the genus and position relative to the fence can considerably affect growth. Therefore, most of the following results are presented using these grouping criteria. A „group“ is the combination of a genus (typically dominated by a single species and represented in the study area by a few species) and position relative to the fence (i=inside, o=outside).

Figure 10 illustrates the significant variation in number of trees analyzed per species and approach. The number of samples for the naive dataset displayed shows the maximum of all individuals recorded over the study period. As some individuals died during the study period, the number of trees recorded per year in the naive dataset varied. The stringent approach to only include trees with consistent height data across all years drastically reduced the number of trees for the cleaned and filled dataset.

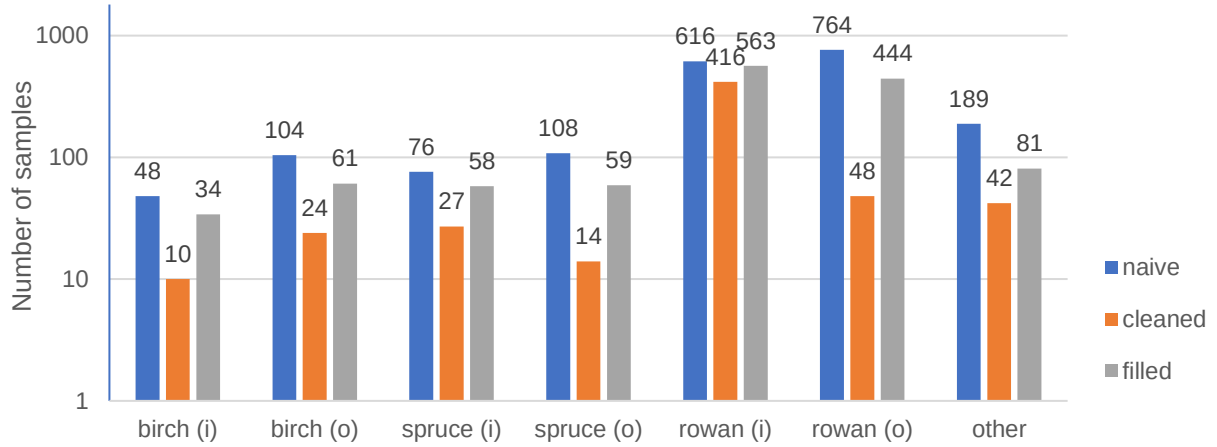

Figure 10: Number of samples used per group and approach (number of samples of tree species not investigated are included in "other", the naive dataset consists of the maximum of all individuals recorded throughout the study period)

For birch positioned inside and outside relative to the fence, as well as spruce located outside the fence, the number of trees in the cleaned dataset was notably low. This dataset included about a quarter of the trees for all groups, with the exception of except for rowan trees. For rowan, the number of individuals was reduced by more than tenfold. Given the notable reduction in dataset size for the cleaned approach an attempt was made to impute missing height data to use a broader dataset that still included trees with complete data across all study years. The filled dataset was approximately twice as large as the cleaned dataset, except for rowan trees inside the fence.

The knowledge about missing data as described in Chapter 3.2 was integrated into the criterion for imputation. Various criteria were tested and their influence on the integrity of the growth data was assessed. The criteria tested and the distribution of tree heights of the different imputed datasets area displayed in Figure A 1. The imputation method identifying trees of the same group (species and position relative to the fence) that had a correlating height growth pattern. For a tree with missing height data in a given year, another tree with the corresponding height data for that year was used to approximate the missing height using a linear regression. The criterion for selecting trees for approximation considered both the coefficient of determination (R^2) and the shared number of height data points across the years by employing the formula:

$$crit = \ln(N) * R^2 \quad (7)$$

with N and R^2 being defined regarding their criteria type

The final criterion used for imputation employed a differentiated approach for birch and all other trees, exploiting the allometric relationship between height and diameter for birch trees to specifically generate missing height data for 2022. For other trees, the criterion was defined to be

stricter due to more available data points for height than for DBH, with measurements of DBH only commencing in 2020.

Figure 11 displays the median height distribution for both the naive and filled approaches.

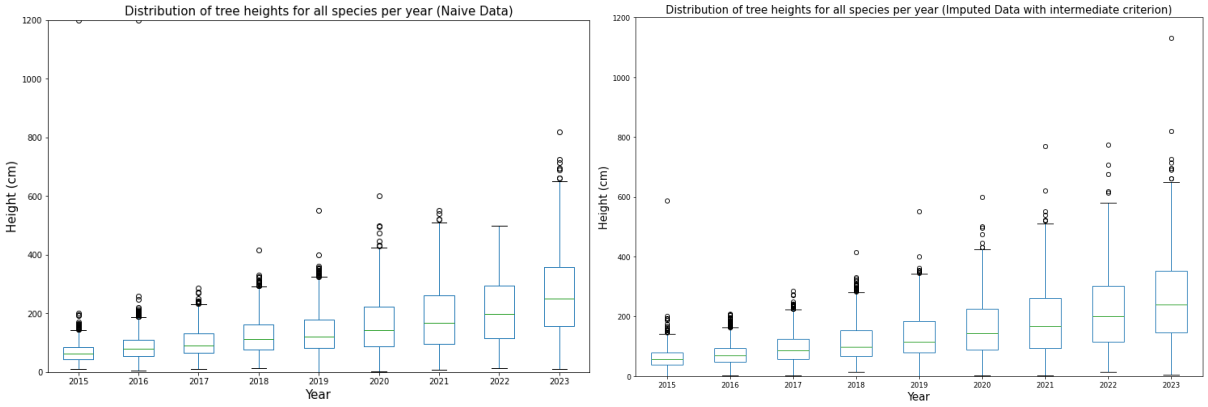

Figure 11: Height distribution for all trees for the naïve(left) and filled (right) dataset

The analysis of the height distribution data from the naive and filled approaches indicates minor shifts in medians and variability, with notable changes in outlier frequency across different years. The symmetry of the boxplots changed with a slight decrease in tree heights for 2018 and an increase for 2021 and 2022. The year 2015, 2021 and subsequent years showed an increase in outliers for the imputed dataset.

The constraints in measurement for anomalies in 2022 and 2023 were reduced through the imputation of missing height data especially for bigger trees. This comparison suggests that the original growth patterns of the trees were largely preserved. Critical for the robustness of the imputed dataset is the influence of interpolation and extrapolation methods. The imputation methodology did not distinguish between interpolation and extrapolation. Extrapolation generally provides less precision, potentially leading to uncertainties for the first and last year. A further improved criterion might mitigate the impact of outliers, as an increase in outliers was observed in 2015 and 2023.

For biomass calculation, the height and diameter data from the filled dataset were used in combination with the functions provided in Chapter 2.1.2. For tree heights below 130 cm, Equation 1 and Equation 2 differentiate between decidiuous and coniferous trees for the different parameters used for biomass calculation. For trees bigger than 130 cm, it distinguishes between different tree species for the different parameters. Only for spruce, species-specific parameters were provided. Birch and rowan were attributed to the category of other decidiuous trees described in Table 1, as there were no species specific parameters provided by Riedel and Kändler (2017).This potentially leads to approximation errors, as the biomass equations are highly species specific. The limited number of birch trees considered in the biomass dataset, might lead

to non-representative results for this species. Figure 12 shows the number of trees that were recorded for the dataset used for biomass estimation in comparison to the naive dataset.

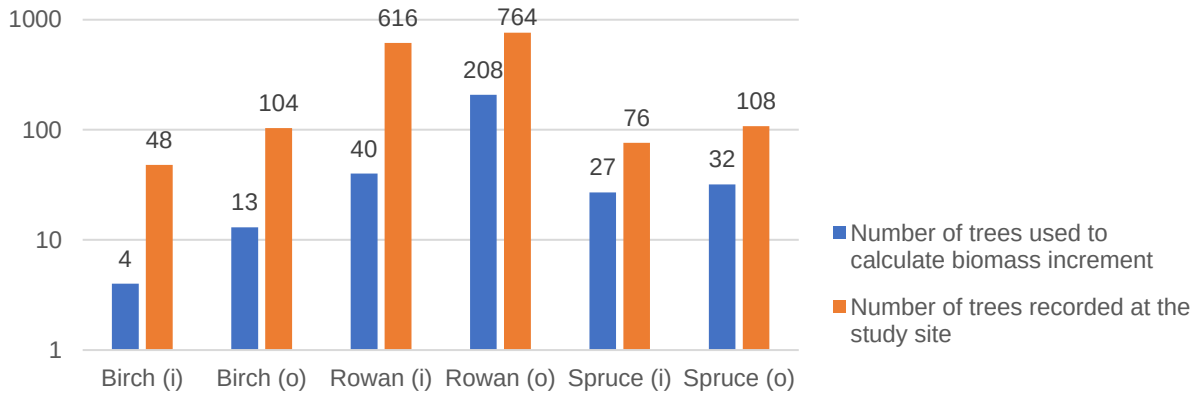

Figure 12: Sample size of biomass dataset and initial (naive) dataset

The dataset employed for biomass calculations represents a small percentage of the total tree population in the study area. Less than 20 per cent of all birch and rowan trees were used. For birch, notably only 4 trees from inside the fence and 13 trees outside the fence were used, constituing to a statistically insignificant sample. For rowan, 40 trees from insde the fence and 208 from outside were used.

Imputation techniques were also employed for the biomass estimation. Missing biomass data was obtained through correlating the height increment of a single tree to its biomass increment and calculating the biomass increment with height data with linear regression. The threshold for imputation were R^2 values obtained from the linear regression above 0.8. Figure 13 illustrates the biomass distributions for the dataset with and without imputation.

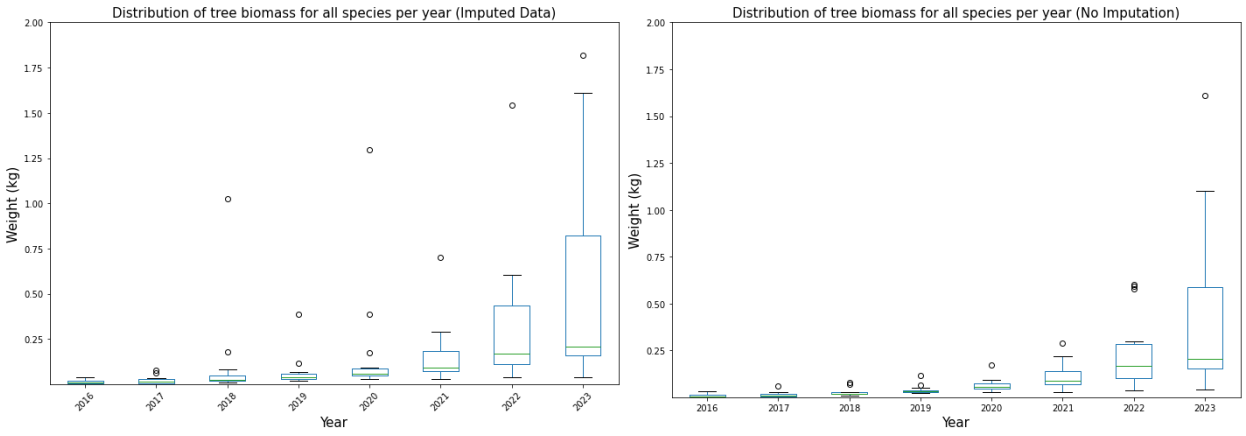

Figure 13: Biomass distribution for all species with imputation (left) and without imputation (right)

For post-imputation, slight changes in the distribution of median biomass could be observed. For all subsequent years from 2018, the interquartile range increased. For the years 2018, 2022, and

2023 more outliers and an expansion of the whiskers were notable, although the median values were consistent.

The increment of biomass after the imputation of missing biomass is displayed in Figure 14.

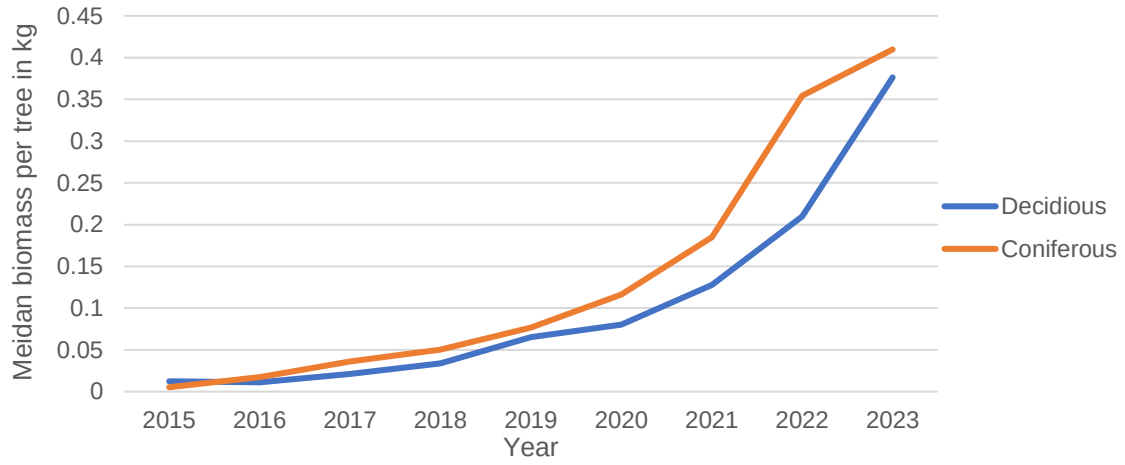

Figure 14: Median biomass increment per tree (imputed dataset)

For deciduous trees, the growth rate of biomass approximates an exponential increase. Similarly, coniferous trees demonstrate an exponential growth with a slightly steeper slope. For the growth in 2023 a notable deviation is observed in the growth rate of coniferous trees. This reduction might potentially be attributed to the felling of spruce by the national park authorities in the beginning of 2024. The logging has potentially biased the dataset as large spruce trees were cut into parts and therefore often impossible to reconstruct. The tree height for small trees that were not cut into parts and trees for which the reconstruction was possible were still present in the dataset of the final year.

4.1.2 Carbon data

The growing season was reported to begin in April with bud formation and ceased in October when no new growth was visible on the branches (*pers. comm.* Alexander Graf). This follows a phenological definition of the growing season. As another factor for defining the growing season, cumulative GPP fluxes per day derived from EC measurements were analyzed for the study period. GPP was used as a proxy to identify the majority of photosynthetic activity and therefore assess the period of major carbon sequestration (Körner et al. 2023). Months were identified based on the criterion that their median number of days with GPP fluxes fell below the 25th percentile for one day.

Figure 15 displays the distribution of days with GPP fluxes below the 25th percentile for the different months throughout the study period.

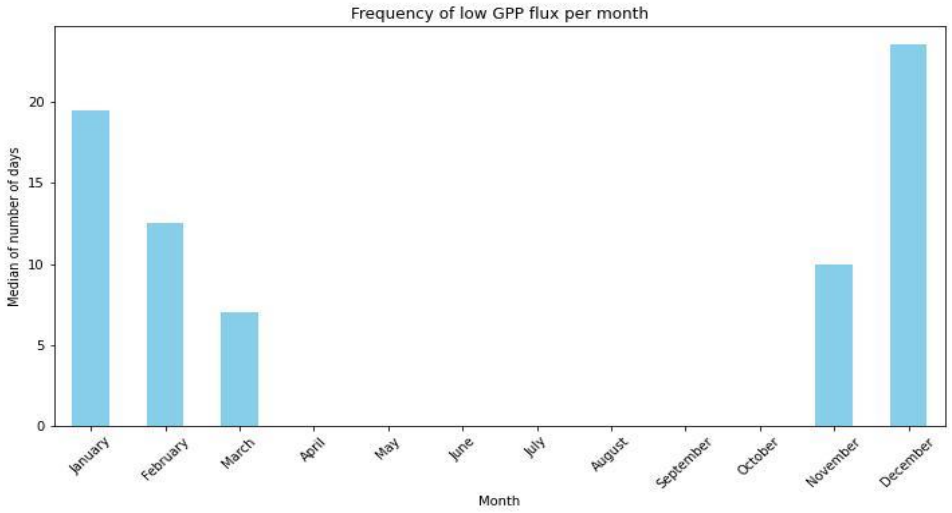

Figure 15: Frequency of days with GPP fluxes below the threshold of the 25th percentile

The months of November to March were identified to fall below the threshold. This supported the initial report on the observed growing season. Therefore, the growing season considered for the carbon fluxes, was defined from April to October.

For the growing season defined, the range of cumulative NEP was from -86 g C m^{-2} yr^{-1} to 216 g C m^{-2} yr^{-1} for the study period.

4.2 Linking tree height increment with NEP and GPP

As a first attempt to assess the relationship between carbon uptake and tree growth, a correlation analysis for the absolute tree height increment and NEP for the study period was performed. Because there was a sufficient sample size for rowan trees in 2016, tree data from that year was only included for rowan trees.

This section focuses on the groups described in 4.1.1 Tree data. As to the scope of the study, only the selected species were analyzed. However, the correlation coefficients for all species present in the study area can be found in the Appendix in Figure A 2, which employs the same differentiation into groups.

Pearson correlation analysis demonstrated a notable variability in the strength of correlations between height increment and NEP depending on the species and location relative to the fence. The highest difference for the resulting correlations was found for rowan trees located outside the fence due to the approach.

The various coefficients for the groups and per approach are shown in Figure 16.

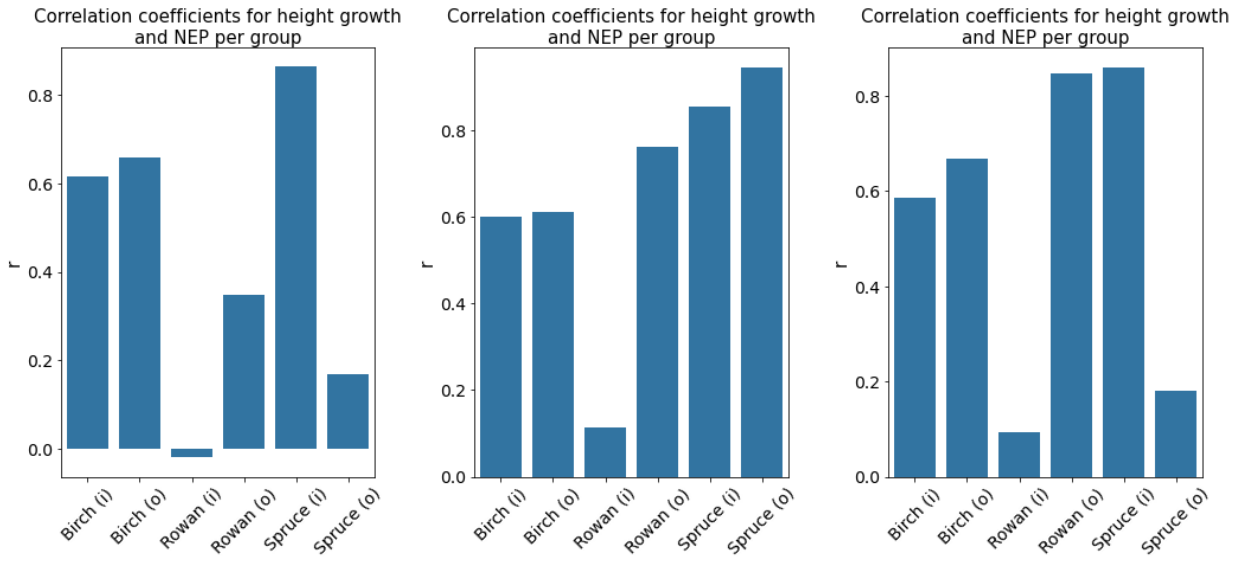

Figure 16: Pearson correlation coefficient for height increment and NEP fluxes per group for the different approaches (left: naive dataset, middle: cleaned dataset, right: filled dataset)

A notably strong correlation was observed for spruce located inside the fence across all approaches, with r=0.86. Spruce outside the fence showed a very weak correlation of 0.17 for the filled and naive approach. For the cleaned approach, a strong relationship was found for spruce located outside the fence with a Pearson coefficient of 0.95.

Birch located outside the fence showed a moderate to strong correlation with coefficients above 0.6. For birch inside the fence, the Pearson correlation coefficients demonstrated slightly weaker relationships compared to the birch comparison group. For the cleaned approach, the position of birch relative to the fence did not impact the observed correlations.

The correlation for rowan inside the fence was very weak for all approaches, ranging from - 0.02 to 0.12. For rowan trees outside the fence, the correlation coefficients varied depending on the approach. For the cleaned and filled approaches, a strong correlation could be found with r = 0.76 and 0.85. For the naive approach the correlation was moderate with 0.35.

The correlation coefficients employing Spearman rank method can be seen in Figure 17.

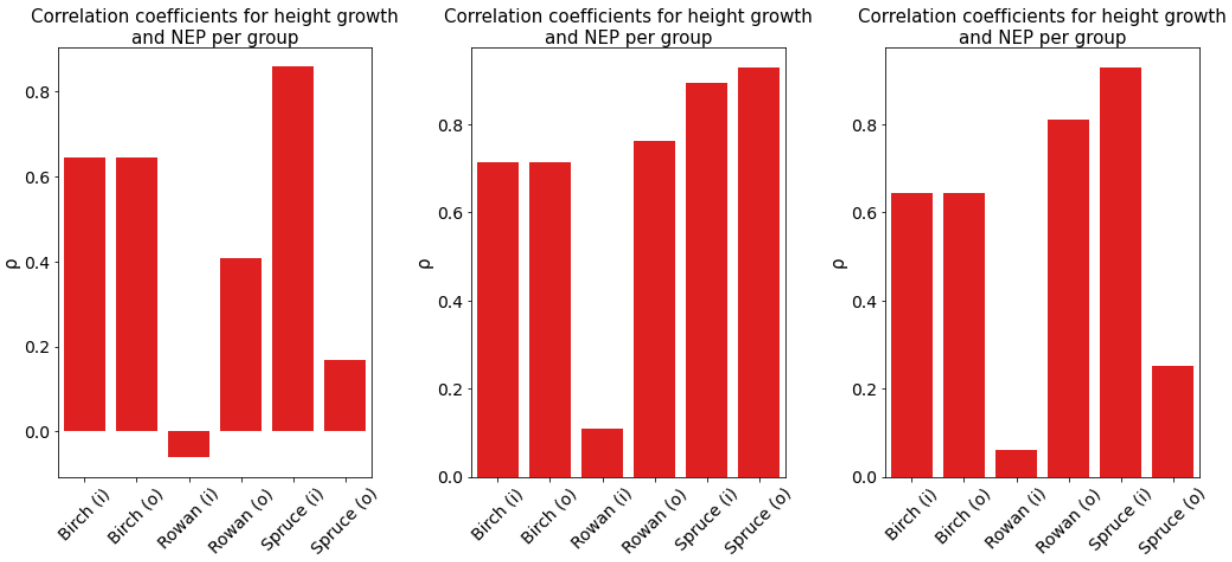

*Figure 17: Spearman correlation coefficient for height increment in cm and NEP fluxes in g*C/(m²yr) per group for the different approaches (left: naive dataset, middle: cleaned dataset, right: filled dataset)*

When employing the Spearman correlation, birch trees continued to show a strong correlation similar to the Pearson coefficient with ρ=0.64 irrespective of their location relative to the fence for the naive and filled approaches. The cleaned dataset demonstrated a higher Spearman coefficient compared to the Pearson coefficient for birch trees. The correlation for spruce inside the fence stayed consistent, showing the same results as for Pearson. The correlations for spruce outside the fence and rowan were similar to the results obtained through Pearson coefficients.

For the cleaned dataset, the results for the group spruce outside and all birch trees indicate limited reliability due to the small sample sizes. The sample comprised only 14 individuals for the group of spruce that was located outside the fence and 10 birch individuals for the respective inside group. Therefore, the differing results for these species can be assumed to be limitedly representative.

High correlation coefficients were observed for most tree groups, except for rowan trees located inside and spruce located outside the fence. The difference in results for spruce inside and outside might point to factors such as browsing to notably impact tree growth, which is not considered in the relationship between carbon uptake and height increment. For rowan, opposite results were obtained with rowan outside the fence demonstrating higher correlations. This disparity suggests additional variables such as differences in soil conditions, competition and water availability, to account for the observed differences.

The relatively short observation period of seven years (for the rowan population respectively eight years), might not represent the long-term forest dynamics of the study area adequately.

4.3 Linking tree biomass increment with NEP and GPP

The correlation analysis for NEP and biomass increment showed distinct patterns in the relationship for different tree species. The plots for Pearson coefficients and Spearman coefficients are displayed in Figure 18.

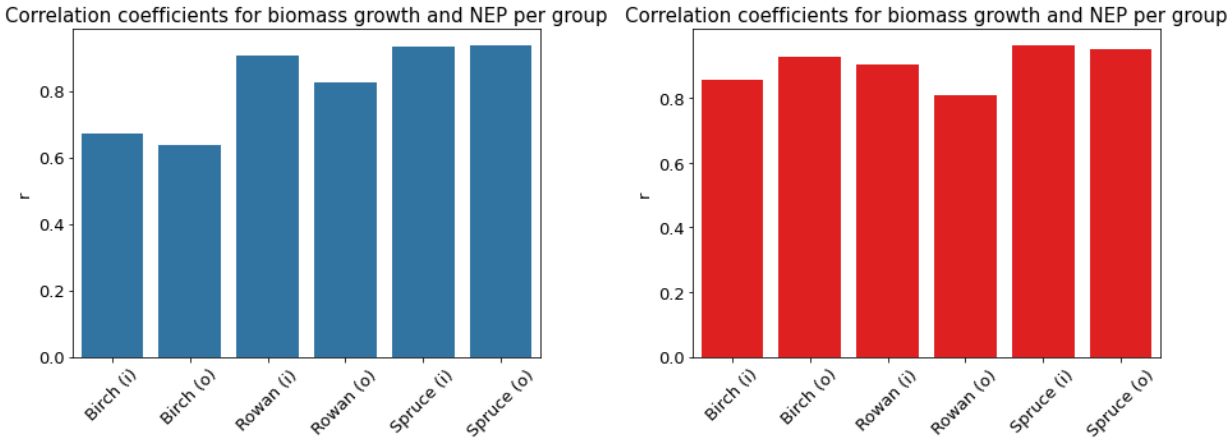

Figure 18: Correlation coefficients for biomass increment and NEP fluxes per group (left: Pearson coefficient, right: Spearman coefficient)

Using Pearson correlation, a strong relationship between biomass increment and NEP could be observed for spruce and rowan, irrespective of their location to the fence. The correlation coefficients for both spruce groups and rowan located inside the fence were shown to be notably high, with values exceeding 0.9. For rowan located outside the fence, a high correlation with a Pearson coefficient of 0.82 was demonstrated. The birch groups demonstrated lower correlation coefficients compared to the other tree species. Notably for the deciduous species, the Pearson coefficients were higher for groups located inside the fence compared to those outside for the same species. For spruce, the correlation coefficient was higher for the group located outside the fence. As reported in Section 4.1.1, browsing had a more pronounced impact on deciduous trees at the study site, which may have influenced the results.

The Spearman coefficients demonstrated strong correlations for all tree species examined. The correlations for spruce and rowan trees remained relatively stable in comparison to the Pearson coefficients. The correlation for birch trees showed higher coefficients for the Spearman method than Pearson.

Despite the variation in coefficients for birch trees, the overall results were consistent for both correlation coefficients. Given the assumption of a linear relationship between NEP and biomass increment, the results appear reasonable.

Spruce exhibited the strongest correlation coefficients, closely followed by rowan trees, indicating that these species potentially exert the highest relative influence on the footprint of the flux

measurements compared to other species present in the study area as suggested by Teets et al. (2018).

Comparing the relationships between height increment and biomass increment with NEP, stronger correlations were found for biomass increments across most groups. Groups that did not demonstrate a correlation between height increment and NEP, showed strong positive relations for biomass increment and NEP. This change was evident for spruce located outside the fence and rowan located inside the fence. The variations might be attributed to the differences in the number of individuals included in the dataset. As mentioned in Section 4.1.1, the biomass dataset was further reduced, as it was not possible to obtain the biomass measurements for all trees present in the filled dataset. Specifically, the discrepancy in the results for rowan located inside the fence may be due to a reduction in the number of individuals from 563 in the filled dataset to 40 in the biomass dataset. For spruce trees located outside the fence, the reduction in the number of trees to 32 individuals in the biomass dataset, could have influenced the observed changes. The limited selection may have likely influenced the results, as the growth dynamics of the selected trees might differ from those of the whole population. The total number of birch trees was limited to 17 individuals in total for both locations, necessitating a careful interpretation of the results.

As the study relied on biomass estimation through field measurements and the use of biomass functions, several constraints were introduced that impacted the accuracy of the results.

- Measurement Techniques:

This study employed conventional tree measurements instead of continuous monitoring techniques such as tree dendrometers, which were used in comparable studies provided in Chapter 2.4 (Granier et al. 2008; Lagergren et al. 2019; Teets et al. 2018) Through field measurements, tree height and diameter were recorded in the non-growing season (September to April). This timing potentially limited the precision of our growth analyses.

- Employment of biomass functions:

The study employed a linear approximation method to derive the diameter at 30 percent of tree height for Equation (2 by relating DBH and diameter at a height of 10 cm. This serves as a proxy and establishes a linear relationship between the height and diameter measurements, whereas the relationship might not accurately portray the vertical profile of tree trunk diameter.

- Diameter variability:

Diameter measurements were influenced by natural fluctuations, which follow annual and diurnal cycles. Variations in stem diameter are mainly influenced by temperature, precipitation, and radiation (King et al. 2013). Air temperature is a significant factor affecting diameter size variations. This intra-annual variability is illustrated in Figure 19, displaying the change in diameter together with temperature changes.

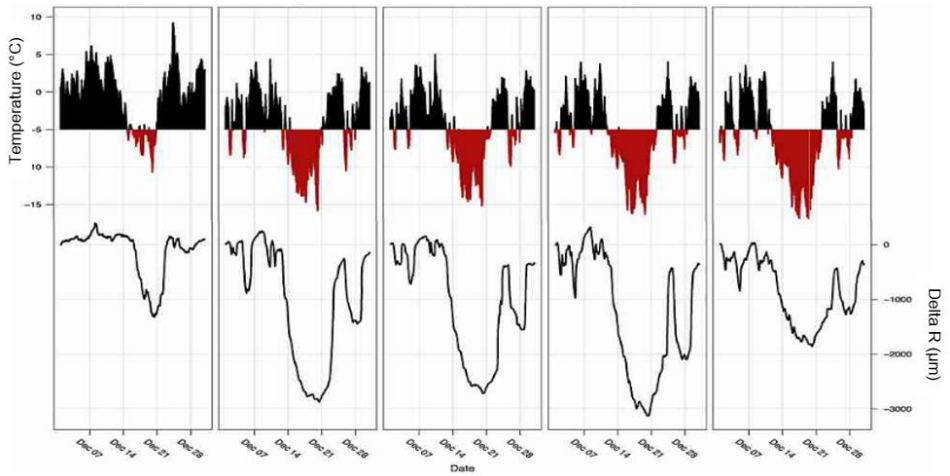

Figure 19: Intra-annual variability of tree diameter relative to air temperature on different elevation sites (increasing elevation from left to right) (King et al. 2013)

During winter months, decreases in diameter are linked to freezing events (temperatures below – 5°C), resulting in a reduction in stem radius range of one to three millimeters less (King et al. 2013). This is caused by extra-cellular freezing, which leads to osmotic water movement of intra cellular water starting below the sap's freezing point (King et al. 2013).

In contrast, precipitation is linked to a diameter increase in the growing season (King et al. 2013). As the biometrical measurements were not made during the growing season, it did not notably affect the results.

- External factors:

The final year of height and diameter measurements was affected by the National Park administration's decision to cut down all spruces, leaving them onsite. Larger spruce trees were sectioned into parts, which led to difficulties in assessing the height. For many large individuals, it was not possible to reconstruct them. As a result, potentially larger spruces were excluded from the biomass calculation data, which is a deviation from the expected growth patterns due to the management practices.

- Constraints for comparison

The carbon intake period was defined based on the observed growth phases at the study site to begin in April with bud formation, serving as a marker for aboveground biomass growth. This approach varies in the literature, which complicates the comparison with other studies due to methodological differences. However, as the fluxes are recorded at 30-minute intervals, the measurements can be adapted to different periods.

To enable a direct comparison between biomass increment and NEP, biomass increments were adjusted by a species-specific carbon content factor and expressed on a stand-level per area basis. The carbon content factors were obtained from the 2021 Wood C Database by Doraisami et al. (2021) if data was available. Specific carbon content measurements for rowan and spruce were sourced from different forests in Germany (Thomas and Martin 2012; Wolff et al. 2009). For birch, an average from the values provided in the database was used as there were no measurements for a German forest (Doraisami et al. 2021). Table 5 provides the carbon content per tree species:

Table 5: Carbon content per species

Tree species	Carbon content [%]
Birch	46.88 (Doraisami et al. 2021)
Rowan	48.20 (Wolff et al. 2009)
Spruce	50.42 (Thomas and Martin 2012)

To obtain annual total carbon flux, the median carbon growth per year for the selected tree groups was multiplied by the total number of trees throughout the observation period. The areas inside and outside the fence were measured using QGIS, which approximates the actual area based on sparse reference points for the fence. The division into areas is displayed in Figure 5 in Chapter 3.1. The areas inside and outside the fence were measured to be 5732 m^2 and 6444 m^2 respectively, comprising a total area of 12176 m^2.

Figure 20 depicts the regression curves linking biomass increment and NEP for the growing season. One analysis differentiates into genus and location (left), whereas the other two analyses demonstrate the regression curves for the two variables for the inside population and outside population relative to the fence (middle and right).

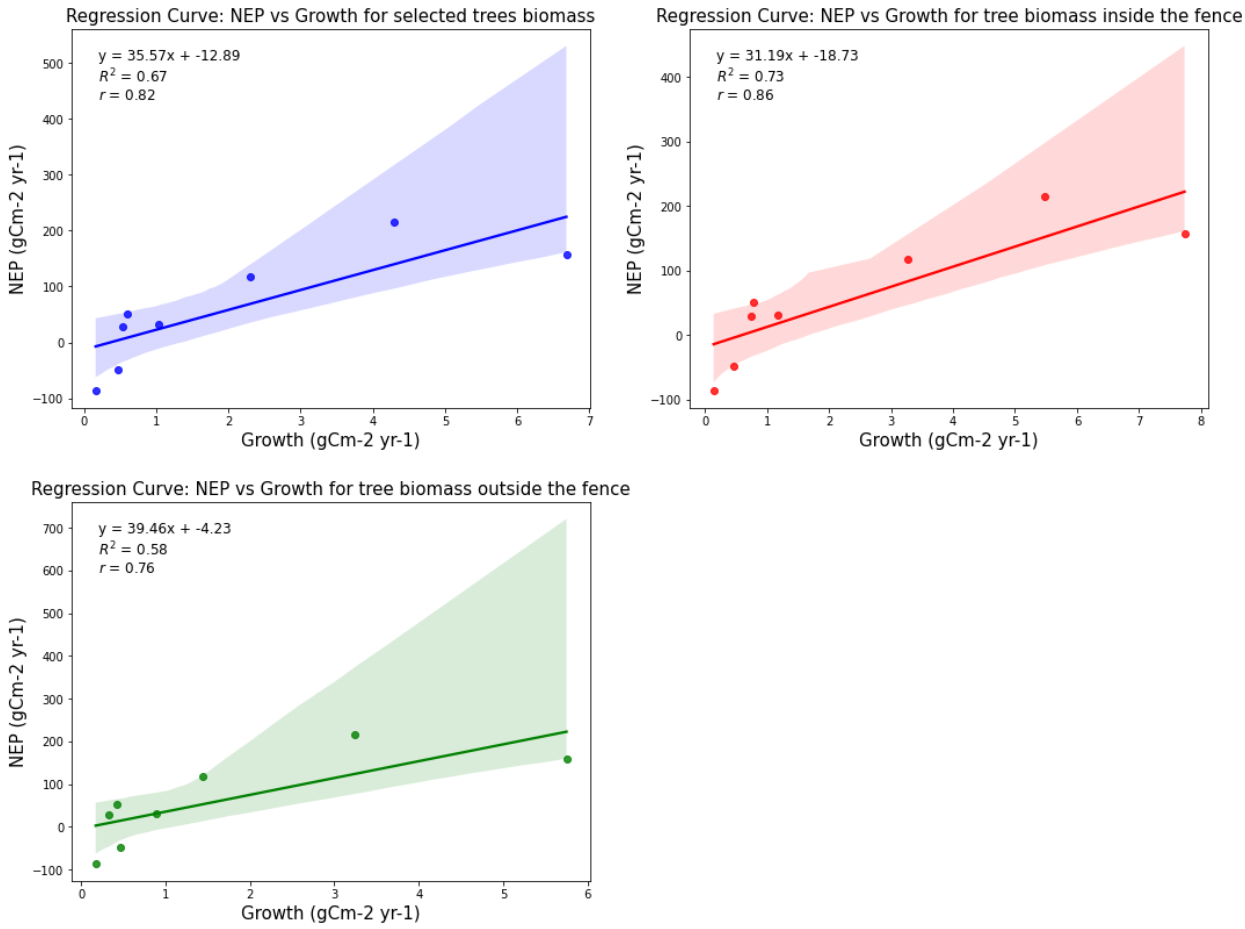

Figure 20: Regressions curves for biomass increment and NEP for the growing season (blue= investigated tree species, red= investigated trees inside the fence, green= investigated trees outside the fence) with the shaded area indicating the 95 % intervals

All three regression analyses indicate strong correlations between the biomass increment and NEP flux for the growing season. The highest Pearson coefficient can be observed for the correlation between biomass increments for the area observed within the fence and NEP flux with 0.86. The correlation coefficient for the tree population outside the fence was found to be smaller compared to those inside the fence, with r=0.76. As a result, the overall correlation coefficient for all sampled individuals at the study site, which is limited to the selected species, was found to be 0.82. The coefficient of determination exhibited the lowest value for the correlations of the tree population outside the fence, indicating that the model has limited predictive ability for the variability in the data of this group.

The regression slopes indicate that approximately 2.5 % (1/40) to 3.3 % (1/30) of the total vegetation period C influx measured by EC was stored in the aboveground biomass of the selected tree species.

The variability in carbon flux magnitudes between the biometrical and EC methods is influenced by the exclusion of belowground biomass and other vegetation other than that of birch, rowan and spruce trees. Lower biomass increment relative to NEP, could be also explained with carbon

allocation to reproductive tissues (Mund et al. 2010), fine root production (Gaudinski et al. 2000) and microbial symbionts (Schiestl-Aalto et al. 2019). Furthermore, non-biological carbon losses may also cause differences in NEP magnitudes from tree biomass increment, as they are not accounted for in NEP measurements (Teets et al. 2018).

Potential biases could arise from using a sample of the population for initial biomass calculations and using the median increment paired with the total number of trees recorded over the observation period. Using a share of the entire population for estimating the biomass might not accurately represent the growth dynamics of the whole plot.

Previous studies have documented varying carbon allocation patterns, resulting in temporal mismatches between NEP and biomass increments (Teets et al. 2018; Teets et al. 2022). Different carbon allocation patterns were found between species (Kozlowski 1992; Michelot et al. 2011; Epron et al. 2012) and throughout different tree development stages (Genet et al. 2010).

Teets et al. (2018) observed that shifting the NEP summation from the traditional calendar year to a September to August timeline, enhanced the resulting correlation between NEP and biomass increment for a coniferous forest. This adjustment to the reference period revealed a lag between biomass growth and carbon uptake, which diminished throughout the study. Increasing average spring temperatures might have contributed to this change (Teets et al. 2018), displaying that tree growth appears to be limited more by climate variables than by carbon availability (Körner 2003). Further studies highlight the importance of forest productivity in linking NEP fluxes to biomass increments (Teets et al. 2022). Productivity refers to the visible increment in biomass, suggesting that sites with higher biomass increments are more productive (Teets et al. 2022).

Unfavorable conditions such as drought, might shift the carbon allocation from the formation of carbohydrates to belowground storage (Klein et al. 2014; Hartmann et al. 2015). This emphasizes a tradeoff between storage and growth for a different set of environmental conditions (Teets et al. 2018). Wood formation is considered to be more temporarily restricted than photosynthesis on an annual basis (Rossi et al. 2006) (Körner 2015).

Teets et al. (2022) also noted a lag in carbon allocation in different North American forests, which was more evident for productive forest sites (Teets et al. 2022). For a low-productivity forest, the biomass increment showed a strong relationship with the current annual NEP. This seemed to correlate more strongly with the current year's climate conditions (Teets et al. 2022).

Further investigations by Lagergren et al. (2019) support these findings, as they discovered the highest correlations when the annual period of cumulative NEP was shifted 6-9 months backward from the start of the calendar year for a boreal forest (Lagergren et al. 2019). Granier et al. (2008) found that the seasonal cumulative NEE from May to June strongly correlated with beech tree

growth in northeastern France (Granier et al. 2008). Babst et al. (2014) demonstrated a strong early growing season correlation between biomass increment and NEP, noting that carbon sequestered between January and June is mainly attributed to volume increase. In contrast, carbon sequestered between August and September is used for cell wall thickening and storage (Babst et al. 2014). When at least one month of the growing season was part of the cumulative NEP for the year, biomass increment and NEP showed the highest correlations (Babst et al. 2014).

Difficulties arise in comparison with these, as other studies investigated mature forests, that were net carbon sinks for the whole study period. The study site shifted however from being a net carbon source to a net carbon sink in the middle of the observation period.

In the following Figure (Figure 21), the analysis above (Figure 20) is repeated with an annual NEP flux from measurements between September of the previous growing season to August of the current growing season. This approach uses a shifted reference period for cumulative NEP fluxes to calculate the correlations between NEP and biomass increment and follows the reference period employed by Teets et al. (2018):

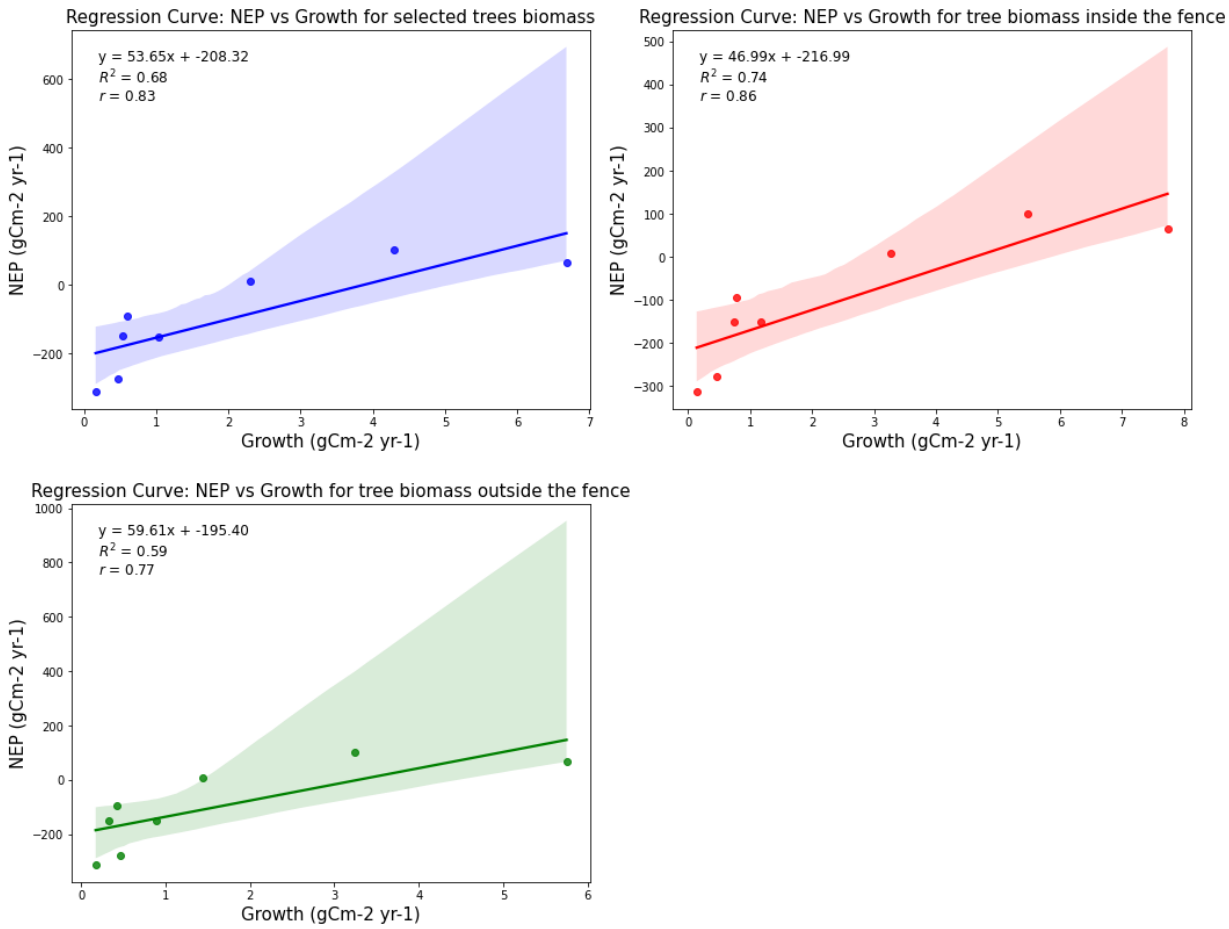

Figure 21: Regression curves for biomass increment and lagged annual NEP from September to August (blue= investigated tree species, red= investigated trees inside the fence, green= investigated trees outside the fence)

The adjustments to the NEP time period resulted in only minor changes, maintaining high correlations. In these regression analyses a notable smaller fraction of the carbon influx was sequestered in the aboveground biomass of the three specie studies – ranging from 1.6 to 2.1 %. The coefficient of determination stayed comparable to the regression analyses for the growing season referenced NEP flux for all groups studied. These results are not conclusively explainable and require further investigation.

Although the results clearly demonstrate a connection, they also underscore the complexity involved in interpreting tree growth dynamics (Teets et al. 2018). As stated by Babst et al. (2014) and Lagergren et al. (2019), understanding the allocation mechanisms in trees is essential (Lagergren et al. 2019). Weather-induced variations in respiration and variable carbon allocation between stem and other tissues seem to play an important role in the variability of carbon uptake and biomass increment (Bouriaud et al. 2005; Litton et al. 2007).

Carbohydrates are used for the synthesis of defensive chemicals against fungi, herbivores and competing plants and as structural elements. These carbohydrates accumulate during periods of high photosynthesis and are depleted otherwise as they are used more rapidly than they are produced, through processes such as respiration, leaching, exudation, secretion, and losses to parasites (Kozlowski 1992). Climate change may further alter these dynamics by changing carbon allocation patterns in trees with varying effects for different bioclimatic regions (Lindner et al. 2010). Warmer temperatures might promote root and foliage growth due to an earlier start to the growing season (Kalliokoski et al. 2012; Lapenis et al. 2013).

Differences in the estimated carbon sequestration could be attributed to unaccounted factors such as belowground biomass increments or the mortality of trees within the study period. Moreover, the reliability of EC measurements may be compromised by inadequate capture of nocturnal respiration, which relies on turbulence that is often suppressed during nights with stable atmospheric conditions (Teets et al. 2018). These elements all contribute to the complexities of quantifying and understanding the relationships within forest ecosystems.

4.4 Perspective

For future research, the inclusion of belowground biomass into the biomass increment might improve the accuracy of comparison between total biomass increment and NEP fluxes. For the estimation of belowground biomass, equations provided in the German forest report 2021 could be employed. (BMEL 2021)

The findings suggest that the growing period defined to be from April to October serves as a good proxy, however further research is required to assess the underlying forest dynamics. Incorporating environmental variables such as mean spring temperature or summer precipitation

add to this, despite suggestions by Teets et al. (2022) that these influences are already encapsulated within the biomass increment. Further investigations into the relationship between carbon uptake and tree growth should aim to align study areas and time frames. Exploring different reference periods for biomass increment and NEP could provide further insights into the forest dynamics, especially as it is suggested that the reference periods for NEP fluxes and biomass differs according to different ecosystems.

Advancements in measurement techniques might further enhance the model accuracy. Employing tree dendrometers would help in aligning CO_2 fluxes and biomass increments to the same temporal resolution. Using species-specific biomass functions, as provided by Wolff et al. (2009) for rowan and birch could improve the accuracy in the biomass estimation. As these functions require the specific diameter obtained at a tree height of 10 cm, which for trees above 1.3 meters was not recorded anymore. Further adapting the functions to obtain the 10 cm diameter from DBH measurements might refine the accuracy of biomass estimation. Moreover, employing new technologies to estimate the biomass via remote sensing and GIS might be a possibility to scale the measured biomass estimation for the whole plot that is assessed with the NEP measurements (Vashum and Jayakumar 2012).

Different studies have explored the potentials of laser profiling and the usage of Landsat TM images for estimation of aboveground biomass in different forests (Steininger 2000; Lefsky et al. 2002). Lefsky et al. (2002) suggest that remote sensing might be more successful for successional forests than mature ones. Through the use of lidar remote sensing, they were able to estimate aboveground biomass across different biomes including mature temperate deciduous and coniferous forest, demonstrating its effectiveness (Lefsky et al. 2002). According to Popescu (2007) LIDAR data can be used to precisely measure biophysical parameters such as DBH, to employ them for biomass estimation Popescu. However, limitations arise for very thin trees, as present in the study area, due to current pixel resolution of LIDAR systems employed in forest assessments. The potentials of optical imagery have also been investigated for biomass estimation (Vashum and Jayakumar 2012). This field requires further research.

Integrating soil chamber measurements to record soil respiration might also help in the understanding of the forest dynamics.

5. Conclusion

Forests are crucial carbon sinks that play a vital role in the mitigation of climate change. Maintaining healthy forests through sustainable practices is essential to leverage their natural resilience and carbon sequestration capabilities. This thesis investigated the dynamics within the ecological regeneration site of Eifel National Park over the period from 2016 to 2024. During this period, the area shifted from being a carbon source after clear-cut in 2013 to a carbon sink since 2021. The relationships between tree growth obtained through manual biometrical measurements and carbon fluxes according to eddy covariance measurements were studied, providing several findings.

Strong relationships were observed between height increment per species and growing season-referenced NEP for some groups. However, no relationships were found between these two variables for rowan located inside the fence and spruce located outside the fence. In contrast to that, biomass increments demonstrated strong correlations with growing season-referenced NEP for all species. Notably, correlations between biomass increment and NEP were higher for the tree population within the fence compared to the population outside of the fence, suggesting the impact of browsing potentially playing an important role.

Spruce trees demonstrated the highest correlations closely followed by rowan and then birch, indicating that spruce and rowan have the highest impact on the footprint of the flux measurements. Challenges in measuring NEP accurately may stem from spatial discrepancies, potentially influenced by the predominant spruce population that surrounds the regeneration site and the high number of rowan trees in the study area.

Notably, the regression analysis indicated that only a small fraction of carbon influx during the growing season - ranging from 2.5 to 3.3 % - was stored in aboveground biomass of the three studied species. This suggests the necessity for further refinement in studying both belowground vegetation and other aboveground components such as shrubs.

Adjusting the reference period of cumulative NEP to an annual period from September of the previous year to August demonstrated positive relations between NEP and biomass increment. As for this regression analysis, an even smaller fraction of carbon influx - ranging from 1.6 to 2.1 % - was stored in the aboveground biomass of the three studied species, with R^2 being marginally lower. These findings suggest that further research is needed to fully understand the underlying forest dynamics.

The use of imputation to address missing data was examined for the biometrical tree measurements. Further refinement of these criteria may enhance the estimation of missing values.

Employing species-specific equations for biomass estimations and integrating dendrometers into the biometrical measurements could improve the accuracy of growth measurements.

The findings of this work underscore the need for continued investigation to fully understand the complex forest dynamics of the study site. Such research is very important to further improve the understanding of carbon dynamics.

Publication bibliography

Aguilos, M.; Takagi, K.; Liang, N.; Ueyama, M.; Fukuzawa, K.; Nomura, M. et al. (2014): Dynamics of ecosystem carbon balance recovering from a clear-cutting in a cool-temperate forest. In *Agricultural and Forest Meteorology* 197, pp. 26–39. DOI: 10.1016/j.agrformet.2014.06.002.

Babst, F.; Bouriaud, O.; P., D.; Gielen, B.; Janssens, I. A.; Nikinmaa, E. et al. (2014): Above-ground woody carbon sequestration measured from tree rings is coherent with net ecosystem productivity at five eddy-covariance sites. In *New Phytologist* 201 (4), pp. 1289–1303. DOI: 10.1111/nph.12589.

Bartsch, N.; Röhrig, E. (2016): Wälder im Klimawandel. In : Waldökologie: Einführung für Mitteleuropa. Berlin Heidelberg: Springer Spektrum, pp. 345–358.

BMEL (Ed.) (2021): Waldbericht 2021. Bundesministerium für Ernährung und Landwirtschaft: Referat 513 - Nationale Waldpolitik, Jagd, Kompetenzzentrum Wald und Holz. Bonn.

Bogena, H. R.; Bol, R.; Borchard, N.; Brüggemann, N.; Diekkrüger, B.; Drüe, C. et al. (2015): A terrestrial observatory approach to the integrated investigation of the effects of deforestation on water, energy, and matter fluxes. 58th ed. Science China Earth Sciences (1).

Bösch, B.; Kändler, G.; Rock, J. (2013): WEHAM 2012 – Waldentwicklungs- und Holzaufkommensmodellierung für die dritte Bundeswaldinventur. Deutscher Verband Forstlicher Forschungsanstalten. Sektion Ertragskunde. Jahrestagung. Rychnov nad Kneznou/Tschechien.

Bouriaud, O.; Bréda, N.; Dupouey, J-L; Granier, A. (2005): Is ring width a reliable proxy for stem-biomass increment? A case study in European beech. In *Canadian Journal of Forest Research* 35 (12), pp. 2920–2933. DOI: 10.1139/x05-202.

Chapin, F. S.; Matson, P. A.; Vitousek, P. M. (2011): Principles of Terrestrial Ecosystem Ecology. New York, NY: Springer New York (2).

Chapin, F. S.; Woodwell, G. M.; Randerson, J. T.; Rastetter, E. B.; Lovett, G. M.; Baldocchi, D. D. et al. (2006): Reconciling Carbon-cycle Concepts, Terminology, and Methods. In *Ecosystems* 9 (7), pp. 1041–1050. DOI: 10.1007/s10021-005-0105-7.

Doraisami, M.; Kish, R.; Paroshy, N.; Domke, G.; Thomas, S.; Martin, A. (2021): GLOWCAD: A global database of woody tissue carbon concentrations/fractions [Dataset]. Dryad.

Epron, D.; Bahn, M.; Derrien, D.; Lattanzi, F. A.; Pumpanen, J.; Gessler, A. et al. (2012): Pulse-labelling trees to study carbon allocation dynamics: a review of methods, current knowledge and future prospects. In *Tree Physiology* 32 (6), pp. 776–798. DOI: 10.1093/treephys/tps057.

Foster, J. R.; Finley, A. O.; D'Amato, A. W.; Bradford, J. B.; Banerjee, S. (2016): Predicting tree biomass growth in the temperate-boreal ecotone: Is tree size, age, competition, or climate response most important? In *Global Change Biology* 22 (6), pp. 2138–2151. DOI: 10.1111/gcb.13208.

Gaudinski, J. B.; Trumbore, S. E.; Davidson, E. A.; Zheng, S. (2000): Soil carbon cycling in a temperate forest: radiocarbon-based estimates of residence times, sequestration rates and partitioning of fluxes. In *Biogeochemistry* 51 (1), pp. 33–69. DOI: 10.1023/A:1006301010014.

Genet, H.; Bréda, N.; Dufrêne, E. (2010): Age-related variation in carbon allocation at tree and stand scales in beech (Fagus sylvatica L.) and sessile oak (Quercus petraea (Matt.) Liebl.) using a chronosequence approach. In *Tree Physiology* 30 (2), pp. 177–192. DOI: 10.1093/treephys/tpp105.

Granier, A.; Bréda, N.; Longdoz, B.; Gross, P.; Ngao, J. (2008): Ten years of fluxes and stand growth in a young beech forest at Hesse, North-eastern France. In *Annals of Forest Science* 65 (7), p. 704. DOI: 10.1051/forest:2008052.

Hartmann, H.; McDowell, N. G.; Trumbore, S. (2015): Allocation to carbon storage pools in Norway spruce saplings under drought and low CO2. In *Tree Physiology* 35 (3), pp. 243–252. DOI: 10.1093/treephys/tpv019.

Heilman, K. A.; Dietze, M. C.; Arizpe, A. A.; Aragon, J.; Gray, A.; Shaw, J. D. et al. (2022): Ecological forecasting of tree growth: Regional fusion of tree-ring and forest inventory data to quantify drivers and characterize uncertainty. In *Global Change Biology* 28 (7), pp. 2442–2460. DOI: 10.1111/gcb.16038.

HSLU Hochschule Luzern (Ed.): Korrelation. Available online at https://www.empirical-methods.hslu.ch/entscheidbaum/zusammenhaenge/korrelation/, checked on 13.02.23.

Kalliokoski, T.; Reza, M.; Jyske, T.; Mäkinen, H.; Nöjd, P. (2012): Intra-annual tracheid formation of Norway spruce provenances in southern Finland. In *Trees* 26 (2), pp. 543–555. DOI: 10.1007/s00468-011-0616-0.

King, G.; Fonti, P.; Nievergelt, D.; Büntgen, U.; Frank, D. (2013): Climatic drivers of hourly to yearly tree radius variations along a 6°C natural warming gradient. In *Agricultural and Forest Meteorology* 168, pp. 36–46. DOI: 10.1016/j.agrformet.2012.08.002.

Klein, T.; Hoch, G.; Yakir, D.; Körner, C. (2014): Drought stress, growth and nonstructural carbohydrate dynamics of pine trees in a semi-arid forest. In *Tree Physiology* 34 (9), pp. 981–992. DOI: 10.1093/treephys/tpu071.

Körner, C. (2003): Slow in, rapid out--carbon flux studies and Kyoto targets. In *Science, New Series* 300 (5623), pp. 1242–1243. DOI: 10.1126/science.1084460.

Körner, C. (2015): Paradigm shift in plant growth control. In *Current Opinion in Plant Biology* 25, pp. 107–114. DOI: 10.1016/j.pbi.2015.05.003.

Körner, C.; Möhl, P.; Hiltbrunner, E. (2023): Four ways to define the growing season. In *Ecology letters* 26 (8), pp. 1277–1292. DOI: 10.1111/ele.14260.

Kozlowski, T. T. (1992): Carbohydrate sources and sinks in woody plants. In *The Botanical Review* 58 (2), pp. 107–222. DOI: 10.1007/BF02858600.

Lagergren, F.; Jönsson, A. M.; Linderson, H.; Lindroth, A. (2019): Time shift between net and gross CO2 uptake and growth derived from tree rings in pine and spruce. In *Trees* 33 (3), pp. 765–776. DOI: 10.1007/s00468-019-01814-9.

Lapenis, A. G.; Lawrence, G. B.; Heim, A.; Zheng, C.; Shortle, W. (2013): Climate warming shifts carbon allocation from stemwood to roots in calcium-depleted spruce forests. In *Global Biogeochemical Cycles* 27 (1), pp. 101–107. DOI: 10.1029/2011GB004268.

Lee, H.; Romero, J. (2023): Climate Change 2023: Synthesis Report. Contribution of Working Groups I, II and III to the Sixth Assessment Report of the Intergovernmental Panel on Climate Change. With assistance of (None), K. Calvin, D. Dasgupta, G. Krinner, A. Mukherji, P. W. Thorne et al. IPCC. Geneva.

Lefsky, M. A.; Cohen, W. B.; Harding, D. J.; Parker, G. G.; Acker, S. A.; Gower, S. T. (2002): Lidar remote sensing of above-ground biomass in three biomes. In *Global Ecology and Biogeography* 11 (5), pp. 393–399. DOI: 10.1046/j.1466-822x.2002.00303.x.

Lindner, M.; Maroschek, M.; Netherer, S.; Kremer, A.; Barbati, A.; Garcia-Gonzalo, J. et al. (2010): Climate change impacts, adaptive capacity, and vulnerability of European forest ecosystems. In *Forest Ecology and Management* 259 (4), pp. 698–709. DOI: 10.1016/j.foreco.2009.09.023.

Litton, C. M.; Raich, J. W.; Ryan, M. G. (2007): Carbon allocation in forest ecosystems. In *Global Change Biology* 13 (10), pp. 2089–2109. DOI: 10.1111/j.1365-2486.2007.01420.x.

Martin, B. R. (2012): Chapter 11 - Hypothesis Testing II: Other Tests. In B. R. Martin (Ed.): Statistics for physical science. An introduction. Waltham, MA, Oxford: Academic Press, pp. 221–242. Available online at https://www.sciencedirect.com/science/article/pii/B9780123877604000111.

Mauder, M.; Cuntz, M.; Drüe, C.; Graf, A.; Rebmann, C.; Schmid, H. P. et al. (2013): A strategy for quality and uncertainty assessment of long-term eddy-covariance measurements. In *Agricultural and Forest Meteorology, vol. 169*, pp. 122–135. DOI: 10.1016/J.AGRFORMET.2012.09.006.

Michelot, A.; Eglin, T.; Dufrêne, E.; Lelarge-Trouverie, C.; Damesin, C. (2011): Comparison of seasonal variations in water-use efficiency calculated from the carbon isotope composition of tree rings and flux data in a temperate forest. In *Plant, Cell & Environment* 34 (2), pp. 230–244. DOI: 10.1111/j.1365-3040.2010.02238.x.

Mund, M.; Kutsch, W. L.; Wirth, C.; Kahl, T.; Knohl, A.; Skomarkova, M. V.; Schulze, E. (2010): The influence of climate and fructification on the inter-annual variability of stem growth and net primary productivity in an old-growth, mixed beech forest. In *Tree Physiology* 30 (6), pp. 689–704. DOI: 10.1093/treephys/tpq027.

Nakagawa, S.; Freckleton, R. P. (2011): Model averaging, missing data and multiple imputation: a case study for behavioural ecology. In *Behavioral Ecology and Sociobiology, vol. 65* (1), pp. 103–116. DOI: 10.1007/s00265-010-1044-7.

Neumann, M.: Wie reagieren die Bäume auf Temperatur und Niederschlag? In : BFW Praxisinformation, vol. 10, pp. 21–24. Available online at https://bfw.ac.at/030/pdf/1818_pi10.pdf, checked on 14.03.23.

Ney, P.; Graf, A.; Bogena, H.; Diekkrüger, B.; Drüe, C.; Esser, O. et al. (2019): CO2 fluxes before and after partial deforestation of a Central European spruce forest. In *Agricultural and Forest Meteorology, vol. 274*, pp. 61–74. DOI: 10.1016/j.agrformet.2019.04.009.

Popescu, S. C. (2007): Estimating biomass of individual pine trees using airborne lidar. In *Biomass and Bioenergy* 31 (9), pp. 646–655. DOI: 10.1016/j.biombioe.2007.06.022.

Reichle, D. E. (2020): Energy flow in ecosystems. In : The Global Carbon Cycle and Climate Change: Elsevier, pp. 119–156.

Reitz, O.; Graf, A.; Schmidt, M.; Ketzler, G.; Leuchner, M. (2022): Effects of Measurement Height and Low-Pass-Filtering Corrections on Eddy-Covariance Flux Measurements Over a Forest Clearing with Complex Vegetation. In *Boundary-Layer Meteorology vol. 184* (2), pp. 277–299. DOI: 10.1007/s10546-022-00700-1.

Riedel, T.; Kändler, G. (2017): Nationale Treibhausgasberichterstattung: Neue Funktionen zur Schätzung der oberirdischen Biomasse am Einzelbaum. (National greenhouse gas monitoring: New functions for estimating above-ground biomass at single-tree level). In *Forstarchiv* (88), pp. 31–38. DOI: 10.4432/0300-4112-88-31.

Rossi, S.; Deslauriers, A.; Anfodillo, T.; Morin, H.; Saracino, A.; Motta, R.; Borghetti, M. (2006): Conifers in cold environments synchronize maximum growth rate of tree-ring formation with day length. In *The New phytologist* 170 (2), pp. 301–310. DOI: 10.1111/j.1469-8137.2006.01660.x.

Schiestl-Aalto, P.; Ryhti, K.; Mäkelä, A.; Peltoniemi, M.; Bäck, J.; Kulmala, L. (2019): Analysis of the NSC Storage Dynamics in Tree Organs Reveals the Allocation to Belowground Symbionts in the Framework of Whole Tree Carbon Balance. In *Frontiers in Forests and Global Change* 2, Article 17, p. 436278. DOI: 10.3389/ffgc.2019.00017.

Steininger, M. K. (2000): Satellite estimation of tropical secondary forest above-ground biomass: Data from Brazil and Bolivia. In *International Journal of Remote Sensing* 21 (6-7), pp. 1139–1157. DOI: 10.1080/014311600210119.

Teets, A.; Fraver, S.; Hollinger, D. Y.; Weiskittel, A. R.; Seymour, R. S.; Richardson, A. D. (2018): Linking annual tree growth with eddy-flux measures of net ecosystem productivity across twenty years of observation in a mixed conifer forest. In *Agricultural and Forest Meteorology* 249, pp. 479–487. DOI: 10.1016/j.agrformet.2017.08.007.

Teets, A.; Moore, D. J. P.; Alexander, M. R.; Blanken, P. D.; Bohrer, G.; Burns, S. P. et al. (2022): Coupling of Tree Growth and Photosynthetic Carbon Uptake Across Six North American Forests. In *JGR Biogeosciences* 127 (4), pp. 1–20. DOI: 10.1029/2021JG006690.

Thomas, S. C.; Martin, A. R. (2012): Carbon Content of Tree Tissues: A Synthesis. In *Forests* 3 (2), pp. 332–352. DOI: 10.3390/f3020332.

Vashum, K. T.; Jayakumar, S. (2012): Methods to Estimate Above-Ground Biomass and Carbon Stock in Natural Forests - A Review. In *Journal of Ecosystem & Ecography* 2 (4). DOI: 10.4172/2157-7625.1000116.

Wolff, B.; Bolte, A.; Bielefeldt, J.; Czajkowski, T. (2009): Biomasse-und Elementgehalte im Unterwuchs–erste Ergebnisse für Flächen des Forstlichen Umweltmonitorings in Rheinland-Pfalz. Beiträge zur Jahrestagung, pp. 200-212. Edited by DVFFA – Sektion Ertragskunde (Jahrestagung).

Xiao, J.; Zhuang, Q.; Baldocchi, D. D.; Law, B. E.; Richardson, A. D.; Chen, J. et al. (2008): Estimation of net ecosystem carbon exchange for the conterminous United States by combining MODIS and AmeriFlux data. In *Agricultural and Forest Meteorology* 148 (11), pp. 1827–1847. DOI: 10.1016/j.agrformet.2008.06.015.

Appendix

Table 6: Different parameters for the criteria for tree imputation. The criteria was set to the natural logarithm of the number of the shared data points multiplied with the R^2 value of the regression

criterion	weak	intermediate	strict	single
N *(Betula)*	3	3	3	4
N *(all)*	3	4	6	4
R^2 *(Betula)*	0.5	0.5	0.8	0.8
R^2 *(all)*	0.9	0.8	0.8	0.8
ln(N)* R^2 *(Betula)*	0.5493	0.5493	0.8789	1.1090
ln(N)* R^2 *(all)*	0.9888	1.1090	1.4334	1.1090

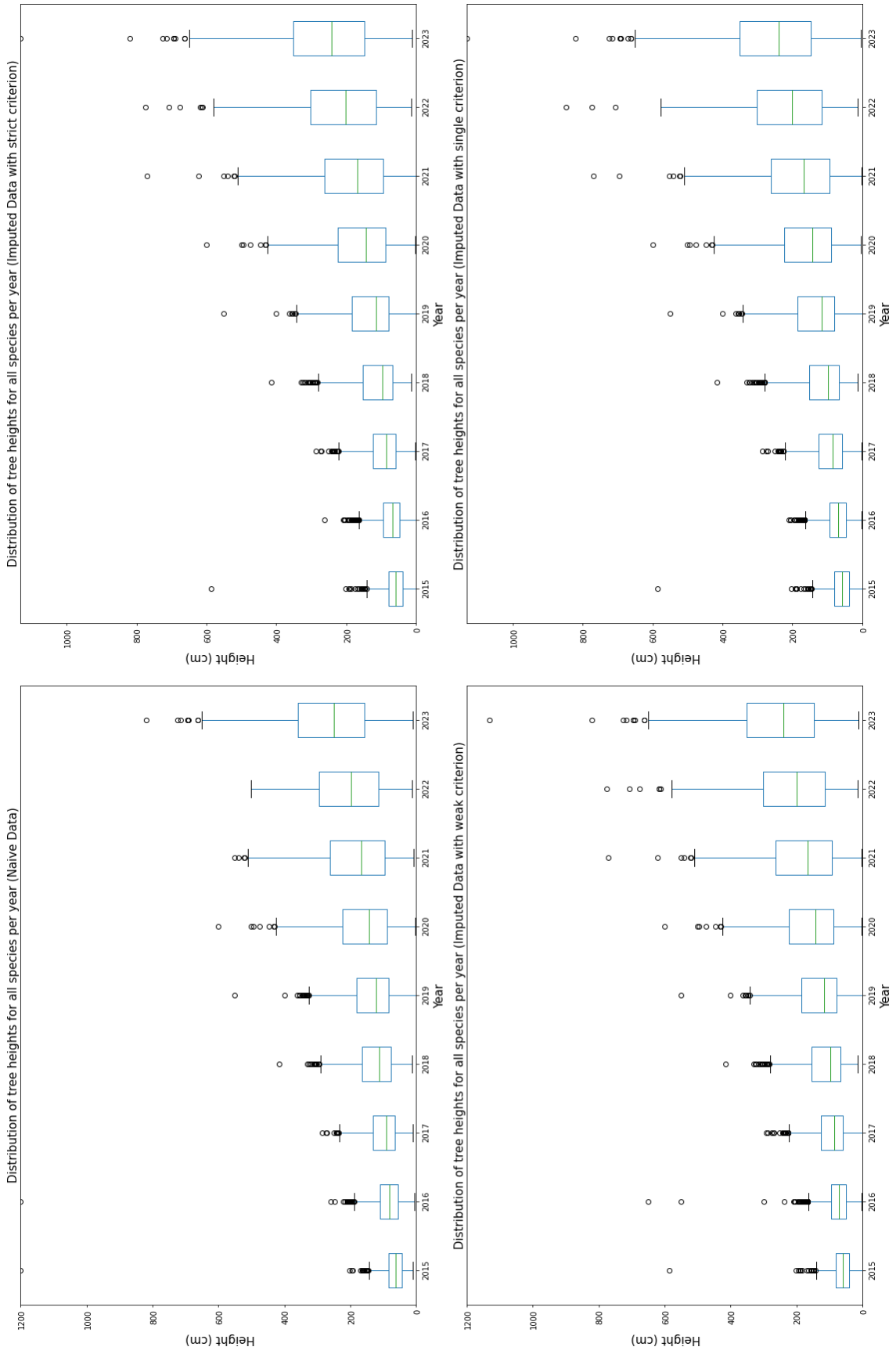

Figure A 1: Distribution of tree heights for the different criteria (upper left: strict criterion dataset, upper right: single criterion dataset, lower left: naive dataset, lower right: weak criterion dataset)

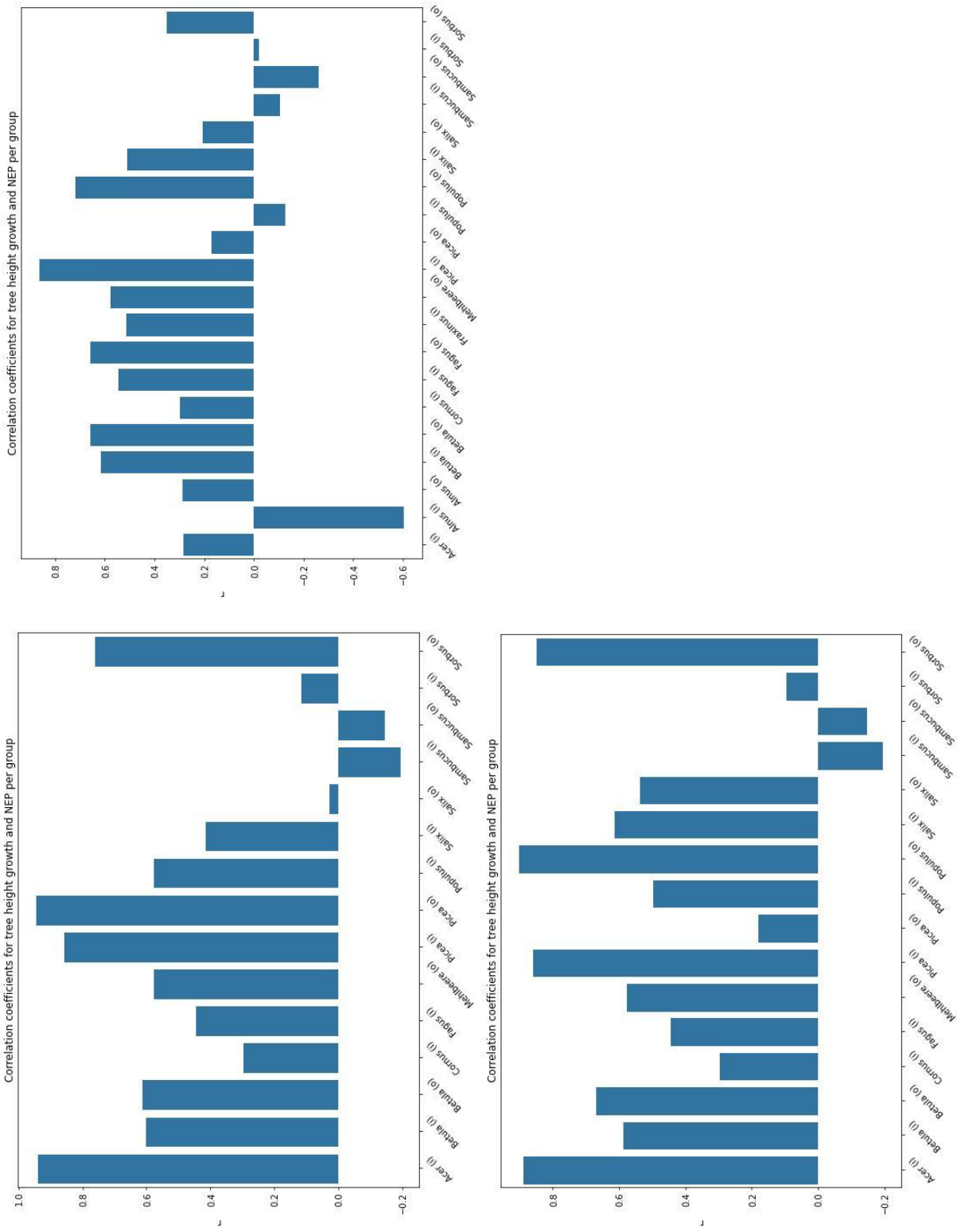

Figure A 2: Pearson correlation coefficients for all groups present in the study area (upper left: naive date set, lower left: cleaned dataset, lower right: filled dataset)